Survey of techniques for improving performance of organic transistors

by

Yu-Mo Chien

A thesis submitted to the Faculty of Graduate Studies and Research in partial fulfillment of the requirements for the degree of Master of Engineering

Department of Electrical Engineering
McGill University
Montreal, Quebec
Canada

August, 2007

Library and
Archives Canada

Published Heritage
Branch

395 Wellington Street
Ottawa ON K1A 0N4
Canada

Bibliothèque et
Archives Canada

Direction du
Patrimoine de l'édition

395, rue Wellington
Ottawa ON K1A 0N4
Canada

Your file Votre référence
ISBN: 978-0-494-38481-7
Our file Notre référence
ISBN: 978-0-494-38481-7

NOTICE:
The author has granted a non-exclusive license allowing Library and Archives Canada to reproduce, publish, archive, preserve, conserve, communicate to the public by telecommunication or on the Internet, loan, distribute and sell theses worldwide, for commercial or non-commercial purposes, in microform, paper, electronic and/or any other formats.

The author retains copyright ownership and moral rights in this thesis. Neither the thesis nor substantial extracts from it may be printed or otherwise reproduced without the author's permission.

AVIS:
L'auteur a accordé une licence non exclusive permettant à la Bibliothèque et Archives Canada de reproduire, publier, archiver, sauvegarder, conserver, transmettre au public par télécommunication ou par l'Internet, prêter, distribuer et vendre des thèses partout dans le monde, à des fins commerciales ou autres, sur support microforme, papier, électronique et/ou autres formats.

L'auteur conserve la propriété du droit d'auteur et des droits moraux qui protège cette thèse. Ni la thèse ni des extraits substantiels de celle-ci ne doivent être imprimés ou autrement reproduits sans son autorisation.

In compliance with the Canadian Privacy Act some supporting forms may have been removed from this thesis.

While these forms may be included in the document page count, their removal does not represent any loss of content from the thesis.

Conformément à la loi canadienne sur la protection de la vie privée, quelques formulaires secondaires ont été enlevés de cette thèse.

Bien que ces formulaires aient inclus dans la pagination, il n'y aura aucun contenu manquant.

Canada

Abstract

Organic field-effect transistors (OFETs) with region-regular poly(3-hexylthiophene) (rr-P3HT) as active semiconductor were fabricated and characterized. Various methods for improving device performance were investigated. These methods include: the use of dip coating technique (rather than spin coating), thermal annealing, polymer doping with iron chloride ($FeCl_3$), and stamping of "dry" poly(dimethylsiloxane) (PDMS) stamp before polymer deposition.

Through experimental results, it is clear that thermal annealing increases charge carrier mobility of P3HT OFETs. On average an increase of four times in charge mobility was observed after thermal annealing was performed. Dip coated samples also resulted in higher mobility values than spin coated samples. Highest charge mobility value achieved were was ~0.02 cm^2/Vs for dip coated samples, where as the highest value for spin coated devices was around 6e-3 cm^2/Vs.

"Dry" stamping of a PDMS devices yielded devices with higher mobility values by around 100% compared to unstamped counterparts. These devices also exhibited lower parasitic leakage currents.

Devices doped with $FeCl_3$ did not perform very well. It is suspected that it was increased so much that it became impossible to turn off the devices.

Résumé

Des transistors à effet de champ organiques (OFETs) avec le poly(3-héxylthiophène) régio-régulier (rr-P3HT) comme semi-conducteur actif ont été fabriqués et caractérisés. De diverses méthodes pour améliorer la performance du dispositif ont été examinées. Ces méthodes incluent : l'utilisation de la technique de l'enduit à immersion (plutôt que l'enduit à rotation), du recuit thermique, du polymère dopé de chlorure ferrique ($FeCl_3$), et de l'emboutissage "sec" du poly(dimethylsiloxane) (PDMS) avant la déposition du polymère.

Selon des résultats expérimentaux, il est clair que la méthode du recuit thermique augmente la mobilité des porteurs de charge des OFETs P3HT. En moyenne, une augmentation de la mobilité de charge de quatre fois est constatée après que la technique du recuit thermique ait été accomplie. Les échantillons enduits par immersion ont aussi résulté avec une mobilité de charge plus élevé que les échantillons enduits par rotation. La meilleure mobilité de charge réalisée était autour de 0.02 cm^2/Vs pour les échantillons enduits par immersion, tandis que le mieux résultat pour les dispositifs enduits par rotation était de 6e-3 cm^2/Vs.

Les dispositifs qui ont été "sèchement" emboutis avec une étampe PDMS avant ont rapporté une mobilité de charge autour de 100% plus élevé que les parties non-embouties. Ces dispositifs ont également démontré moins de courants de fuite parasites.

Les dispositifs dopés de $FeCl_3$ n'ont pas fonctionné très bien. La conductivité avait était augmentée tellement, qu'il était impossible d'atténuer les transistors.

Acknowledgements

I would like to thank Dr. I. Shih for his continued help and support throughout the course of my study. I would also like to thank Organic Vision Inc. for some of the materials used. Special thanks are due to the graduate students in the Electronic Devices and Materials lab at McGill University for their encouragement and friendship. I'd finally like to acknowledge the support of my family for whom this would not have been possible.

Table of Contents

1 Introduction

Organic semiconducting devices are rapidly becoming part of our daily life. As such, it is possible that the organic semiconductor industry will experience an even faster growth than what the inorganic semiconductors experienced.

The first generation of organic light emitting displays is already being mass produced and commercialized. On the other hand, circuits implemented using organic semiconductors are not publicly available to the end users yet. They are nonetheless already present in research laboratories around the world in the form of prototypes. This suggests that a lot more effort is required to introduce organic semiconductors into circuit applications for consumer products.

Organic small molecules and polymers promise for inexpensive, disposable and flexible electronics will not be possible unless the performance of organic field-effect transistors is improved to be on par with amorphous silicon (α-Si). However, performance is not the only requirement. Single crystal small molecules transistor devices have already surpassed α-Si in terms of reported charge carrier mobility but are not suitable for commercialization because of the fabrication costs involved. Cost of fabrication is of prime importance for a technology to survive in the industry; therefore, unless there are ways to fabricate small molecule devices at low cost, improving performance of organic polymer devices is a more viable option.

Therefore, this study will involve the survey of various techniques for improving the performance of organic transistors. Deposition techniques such as spin coating and dip-coating will be compared. Some performance improvement techniques are also investigated, these include: annealing step after deposition, polymer doping with iron chloride, and stamping of a "dry" elastomer before the active organic polymer deposition step.

2 Organic Semiconductor Theory

2.1 Background

Organic semiconductors are not a recent discovery. In fact, anthracene crystals were first studied for their dark and photoconductivity back in the early 20th century. A few decades later, electroluminescence of single crystal anthracene was discovered in the 1960s [1]. This discovery triggered a large body of researchers to investigate further and established the basics of optical excitation and charge carrier transport theory in organic crystals. However, several drawbacks prevented organic semiconductors from making into practical applications in these early days. High operating voltage, instability and low current densities were the main drawbacks. Mean while, conjugated organic polymers were made conductive by controlled doping by Chiang *et al* [2], whom part of the group members were awarded the Nobel Prize in Chemistry in 2000 for their work in the field. A decade later, ongoing research efforts in organic semiconductors reached a breakthrough when the first high efficient organic photovoltaic cell was demonstrated [3]. And around the same period, the same group also demonstrated low voltage organic electroluminescent diodes [4]. By the end of the 1980s, organic thin film transistors (OTFTs) were fabricated [5-8]. These series of advancements in the field of organic semiconductors fueled an even larger interest in the subject that is growing to this date. The domain of organic semiconductors has advanced so rapidly in the last decade, that commercial products have already become reality. Notably, the presence of organic light emitting devices (OLEDs) in car audio equipment displays and portable electronic displays is commonly seen. Other applications such as organic photovoltaic solar cells and integrated circuits utilizing organic field effect transistor (OFETs) should also be making its appearance in the market soon.

2.2 Organic Materials

Organic semiconductor materials are divided into two major classes: oligomers (small molecules or short chains) and polymers (long chains). From a processing point of view, these two classes of materials are different. In order to obtain films, small molecule materials are usually deposited by vacuum evaporation or sublimation. On the other hand, polymeric materials are synthesized into a solution and cast into thin films by spin coating, dip coating or printing techniques. From a chemistry perspective however, both types of organic semiconductors are similar.

The basics of organic semiconductors lie in the particular bonding configuration of carbon atoms: the sp^2-hybridized C-atoms. Two bonding structures are present in sp^2-hybridized C-atom bondings. First, a very strong σ-bond between carbon atoms is present on plane of sp^2 orbitals. And then, perpendicular to this plane, a pair of conjugated π-electron systems formed by p_z-orbitals can be found (Figure 2-1a). It is thanks to these π-bonds that we are seeing the semiconducting properties of these organic material systems. Compared to σ-bonding, π-bonding is much weaker; thus, it can give or take energy much easier. Light absorption (photovoltaic) or emission in the visible spectra can be observed in such transitions between π-orbital (bonding) to π*-orbital (anti-bonding) energy levels.

Bonding and anti-bonding orbitals can be thought as the valence and conduction bands equivalent of inorganic semiconductors. In organic semiconductors, these bands are more often referred to as the highest occupied molecular orbital (HOMO) and lowest unoccupied molecular orbital (LUMO). The energy gap between the HOMO and LUMO for π-orbitals is usually in the order 1.5 to 3 eV for organic materials, which is much smaller than the σ-orbitals (Figure 2-1b). Ethene or ethylene is the simplest of such organic molecules consisting of a single pair of C-atoms as illustrated in Figure 2-1. This configuration is present in both oligomers and polymers.

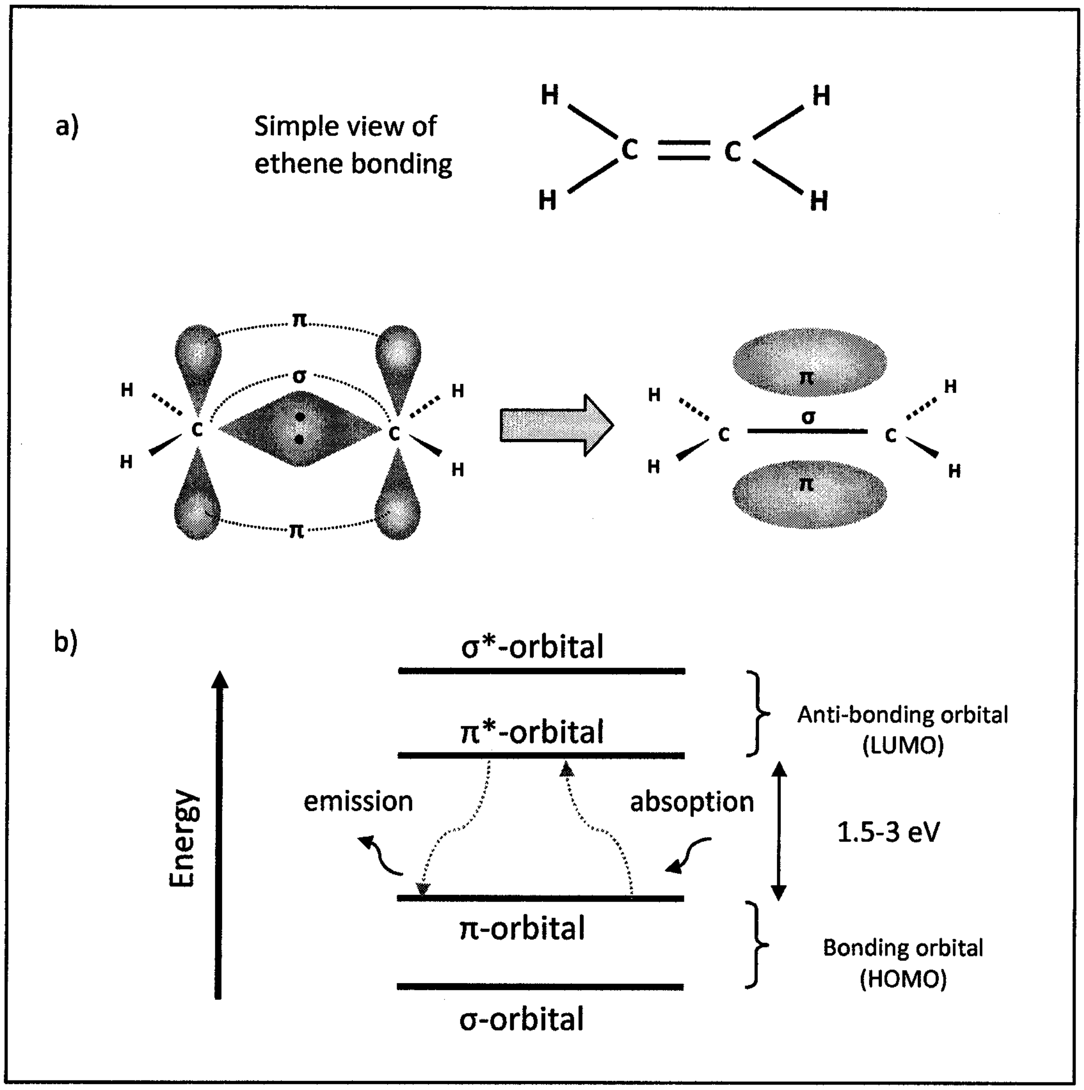

Figure 2-1. Bondings of Ethene.

2.2.1 Organic Small Molecules

Benzene rings are the basic unit in oligomers, consisting of six C-atoms and six H-atoms (C_6H_6) bonded in a ring fashion. In this kind of system, the π-bonds become delocalized; electrons in such bonds are no longer associated to any particular atom or covalent bond. Delocalized electrons are simply contained wthin an orbital that extends over several adjacent atoms. The direct result of these delocalizations is that the energy gap between the LUMO and HOMO of the molecular system becomes smaller; thus giving rise to properties such as conductivity (charge transport).

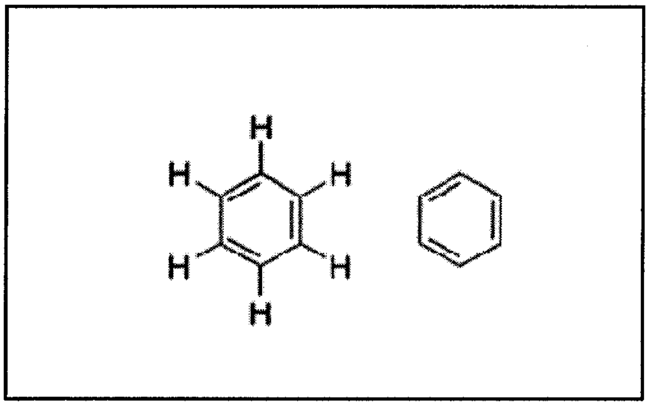

Figure 2-2. Benzene Ring.

Through vacuum sublimation and physical vapor growth techniques [9, 10], it is possible to obtain fairly large single crystals from organic molecular semiconductors (SCO). These crystals exhibit relatively high charge mobility and even show a band like carrier transport due to the highly ordered nature of single crystals; molecules are closely coupled together, allowing the transport of charge carriers with ease. However, SCOs are not suitable for industrial applications because of the costs and time involved in the fabrication of such crystalline materials. Nevertheless, they are essential for carrying out research to investigate the fundamentals governing charge transport in organic conjugated materials. Time-of-flight (TOF) measurements of single crystal organic semiconductors have yielded carrier mobility as large as 400 cm^2/Vs [11], which is similar to electron mobility in Si at room temperature. These results suggest two important facts: organic semiconductors can exhibit band-like carrier transport characteristics; and, the performance of thin-film polycrystalline devices of organic materials is strongly dependent on the purity, or imperfections of the semiconductor itself. Single crystal organic small molecules have also been used to fabricate field-effect devices, and field-effect mobility values obtained range from 0.1 to 20 cm^2/Vs [12] depending on the material and device structure used. These numbers largely exceed even the highest mobility reported for hydrogenated amorphous silicon (α-Si:H) devices.

Figure 2-3 shows some of the most studied organic small molecule semiconductors. As mentioned earlier, anthracene was one of the first organic semiconductors to be studied; however, other molecules in the oligoacene family have been more extensively studied in recent years. Pentacene and tetracene have received particular attention for their higher mobility. Some of their derivatives are also of equal interest such as rubrene, which holds the highest organic semiconductor field-effect mobility value ever reported to date (~20 cm^2/Vs) [13, 14].

For more practical applications, molecular organic semiconductors can also be evaporated in high vacuum to form uniform polycrystalline thin-films. Compared to single crystal organic devices, the thin-film counter parts not only have lower field-effect mobility due to structural defects, but also have a gate voltage dependent mobility. Polycrystalline thin-films do not possess band-like conductivity like SCOs, the transport of carrier is rather accomplished through "hopping". Clearly, organic semiconductor technology has the potential to replace inorganic semiconductors in some areas.

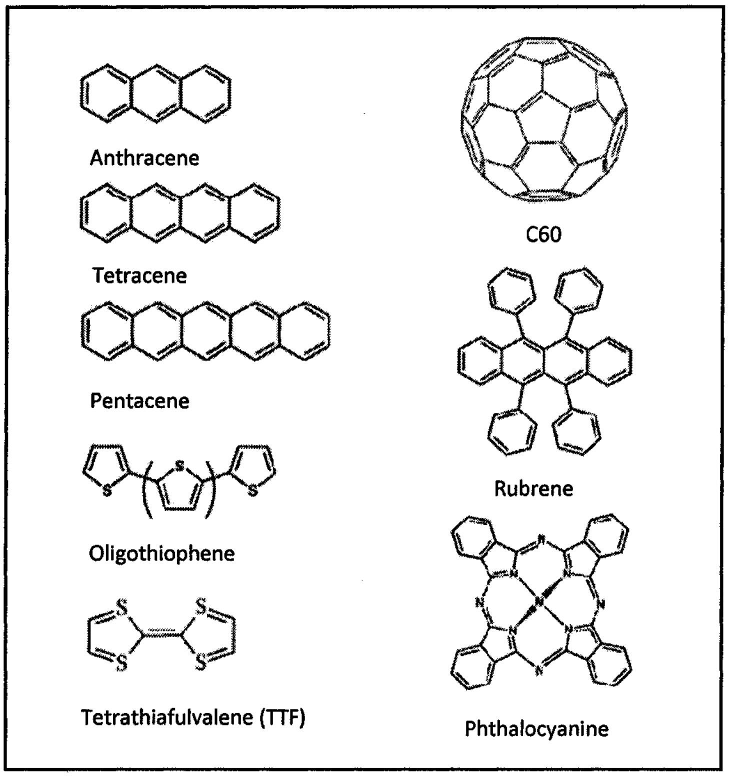

Figure 2-3. Some of the most studied organic small molecule semiconductors.

2.2.2 Organic Polymers

As discussed above, conjugated organic polymers are long chains of carbon atoms. A polymer chain is said to have a one-dimensional electronic system because the delocalization of π-bonds resides along the chain. Unlike organic small molecules, polymeric chains cannot form highly ordered crystals; therefore, charge transport in organic polymers relies on defects along the chains or "hopping" across other polymeric chains. Figure 2-4 shows some of the most commonly studied organic polymers. The depicted chemical structures are single molecules, which can be bonded repetitively n times to form the actual polymeric chain. Polyparaphenylenevinylene (PPV), polyparaphenylene (PPP) and polyfluorene (PF) family of polymers are most often used in light emitting applications where charge carrier mobility is not as crucial as in a high performance OFET. On the other hand, polythiophenes (PT) exhibit the highest charge carrier mobility values among all organic polymers [15]. Field-effect mobility of up to 0.6 cm^2/Vs has been reported for a new semiconducting liquid-crystalline polythiophene polymer [16]. It is known that polythiophenes have a strong tendency to form crystallites through self-assembly when cast into thin films; thus, increasing their charge transport abilities.

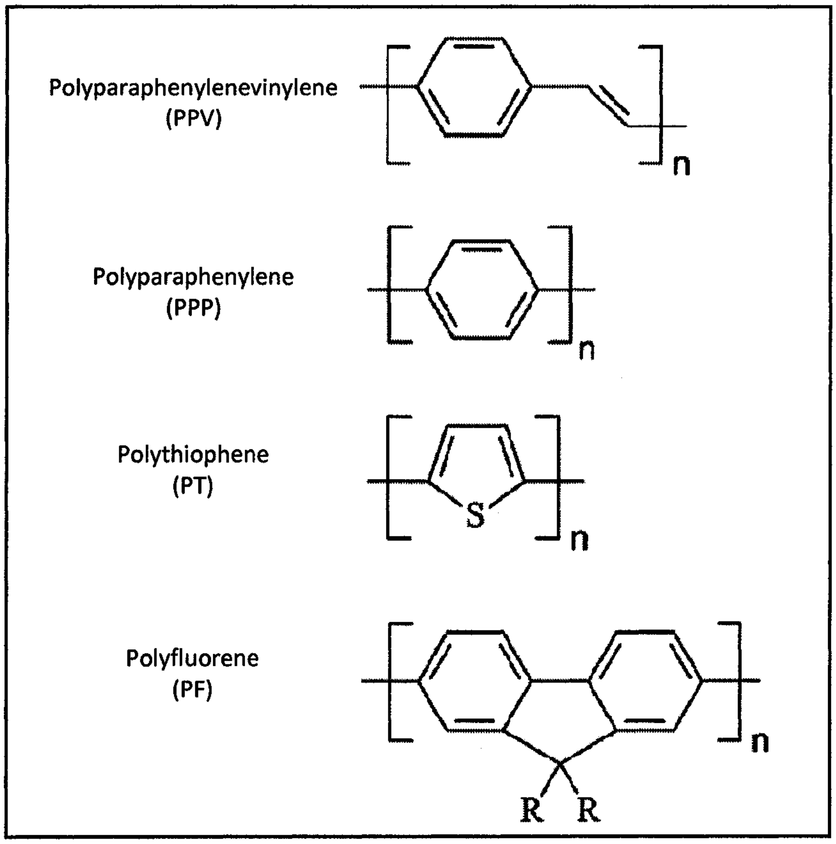

Figure 2-4. Some of the most studied organic polymer semiconductors.

The main advantage of organic polymers over small molecules is their relatively simple fabrication process. Organic polymers are easily dissolved in organic solvents; thus, a solution process can be used for applying organic semiconductors over large areas and flexible substrates with little time and effort.

2.3 Charge Transport in Organic Semiconductors

There is still a lot of controversy for describing charge transport in organic semiconductors. For inorganic semiconductors, charge transport is governed through delocalized states and limited by scattering of the carriers induced by crystal lattice deformations (or phonons) caused by heat. However, if one were to apply this model to low conductivity amorphous organic semiconductors, the estimated mean free path of charge carriers would become smaller than the mean atomic distance, which does not make sense. One the proposed models for describing charge transport in such materials is based on "hopping" of charge carriers between localized states. In this case, the transport is rather assisted and not limited by photons; thus thermally activated.

Polaron is another term used in the description of localized "hopping" of charges. In conjugated organic polymers, localization is caused by polarons, which are the result of a deformation in the polymer chain caused by a charge carrier. Because polymer chains are simply repetitions of monomers in one direction (1D), if a charge carrier is thrown into such structure, the one-dimensional character of the polymer chain could easily be deformed. The model describing transport mechanism of polarons was developed by Holstein in the late 1950s [17, 18].

Another model that attempts to describe charge transport of organic semiconductors is the multiple trapping and release (MTR) model [19]. In this model, a high concentration of localized states, also called "traps", is present in a narrow delocalized band. The transport of charge carriers through delocalized states is then influenced by localized traps. Localized states will trap incoming charges carriers and release them through thermal excitation. This model is currently widely employed for describing charge transport in amorphous silicon.

Besides the temperature dependence of charge transport mechanisms, electric field also becomes important when it exceeds $\sim 10^5$ V/cm. The dependence can be described by the Poole-Frenkel mechanism [20].

It is worth noting that these latter factors affecting charge transport will have different effects on single crystals and amorphous materials. For instance, in SCOs, the mobility will generally decrease as temperature increases; whereas for an amorphous polymer film, it will have a tendency to increase.

2.4 Charge Carrier Mobility

The figure of merit that characterizes the charge transport is the carrier mobility. There are usually two types of carrier mobility that can be found in the literature: intrinsic mobility and the field-effect mobility; the latter is measured when the semiconductor is operated under an electric field (gated device). There are several methods available for estimating these two figures of merit and will be discussed later.

Over the past several years, different organic semiconductor materials have been classified into hole transport (*p*-type) or electron transport (*n*-type) materials. Worth noting however, this classification does not necessarily reflect the intrinsic properties of the materials to prefer the transport of either type of carriers. The carrier mobility reported for the organic materials are most likely limited by the charge injection at the electrodes [21] (eg. How well the electrode work function matches with the organic semiconductor.)

2.4.1 Intrinsic Mobility

Intrinsic carrier mobility quantifies with how much ease charge carriers inside the semiconductor are able to move from molecule to molecule with no disturbance. The most employed methods for extracting this value include time-of-flight (TOF), diode configuration, and pulse-radiolysis time-resolved microwave conductivity (PR-TRMC) [21].

For TOF measurements, an organic material layer is sandwiched between two electrodes. First, an optical pulse from a light source or a laser is directed at the organic material close to one of the electrodes. A layer of charge carriers is then photo-generated by this optical pulse and travels through the sample to the other electrode depending on the bias applied. This response can be measured as a function of time. And the carrier mobility can be calculated using the following equation,

$$\mu = \frac{d^2}{\tau V} \tag{2-1}$$

where *d* is the organic layer thickness, *τ* is the transit time of the charges and *V* is the applied bias voltage.

The diode configuration [22] can be used with the condition that the charge transport is bulk limited and not contact limited. The structure for such configuration is similar to TOF with a layer of organic material sandwiched between two electrodes. Additionally, the electrodes are most often chosen so that only holes or electrons are injected into the bulk at low voltages. When these conditions are met, space-charge limited current will be shown in the J-V transfer curve; the current density will scale with the voltage quadratically. The current density can be expressed with Equation 2-2,

$$J = \frac{9}{8}\epsilon_0\epsilon_r\mu\frac{V^2}{L^3} \tag{2-2}$$

where, L is the thickness and ϵ_r is the dielectric constant of the organic layer. Also, the above equation assumes a trap-free medium, since the transfer curve would be much more complex in the presence of traps.

PR-TRMC is a contact free and the most accurate method for measuring the intrinsic properties of organic semiconductors. The samples are first excited by a pulse of high energy electrons (MeV range), which creates a low density of free carriers in the bulk of the semiconductor. A change in electrical conductivity can then be induced by measuring the change in microwave power reflected from the sample. Equation 2-3 expresses the change in conductivity ($\Delta\sigma$) as a function the sum of electron and hole mobilities and the density of generated electron-hole pairs ($N_{e\text{-}h}$).

$$\Delta\sigma = e\sum \mu N_{e-h} \tag{2-3}$$

The above discussed methods for extracting carrier mobility do not guarantee that the results will reflect the intrinsic mobility of the material. The organic material itself needs to be as pure and as ordered as possible. Organic materials where it is possible to make defect-free crystals out of will have the most accurate results, which further emphasizes the importance of the study of small molecule SCOs.

2.4.2 Field-effect Mobility

While the intrinsic mobility value characterizes the maximum mobility an organic semiconductor has, the field-effect mobility represents the actual performance of the semiconducting material under an electric field perpendicular to the direction of transport, which is generally much smaller than the intrinsic mobility. To extract field-effect mobility, OFETs are fabricated and transfer curves are measured. In 2004, the institute of electrical and electronics engineers (IEEE) defined a standard for testing and characterizing organic field-effect transistors (IEEE Std 1620) [23]. IEEE Std 1620 also includes a standard way of extracting and reporting field-effect mobility for OFET devices. The following is a brief description of the proposed methodology for extracting field-effect mobility.

For the extraction of mobility in the saturation regime of the OFET, Equation 2-4 is used,

$$I_{DS} \approx \frac{W}{2L} C_i \mu (V_{GS} - V_T)^2 \tag{2-4}$$

where I_{DS} is the current through the drain and source electrodes; W and L are the width and length of the transistor channel; C_i is the gate capacitance per unit area; V_{GS} and V_T are the gate voltage and V_T the threshold voltage respectively; and finally, μ is the field-effect mobility. Typically, the most common approach for approximating the mobility value is to plot $I_{DS}^{1/2}$ *vs.* V_{GS} (with V_{GS} at saturation), finding the slope m, and solving for μ. In such case, μ will be given by Equation 2-5,

$$\mu \approx \frac{2Lm^2}{WC_i} \tag{2-5}$$

For the linear operation regime, Equation 2-6 is used for the approximation,

$$I_{DS} \approx \frac{W}{L} C_i \mu (V_{GS} - V_T) V_{DS} \tag{2-6}$$

where V_{DS} (drain to source voltage) has to be << (V_{GS}-V_T). Measuring the transfer I_{DS} *vs.* V_{GS} in the linear region and taking the slope of the curve, one can use the derivative of Equation 2-6 for solving for the mobility.

Although most research groups follow the IEEE standard for reporting field-effect mobility, there are nevertheless many different results for the same polymer among the different laboratories. This is in fact expected, since the charge transport properties of organic polymers depend greatly on the morphology of the material; and morphology itself is influenced by process conditions.

2.5 Organic Field-Effect Transistors

The field-effect transistor (FET) has been the reason behind the success of the semiconductor industry for the past few decades. FETs are simple four terminal devices. Usually, one of the terminals is kept at a constant bias (bulk or substrate). And another terminal (gate) is used to control the current flow through the two remaining terminals (drain and source) by varying the voltage applied. There are several device configurations available for building a FET. The most important one is the MISFET (metal-insulator-semiconductor FET) structure (Figure 2-5). On a MISFET, the gate is isolated from the semiconductor channel by an insulator layer. When a voltage is applied at the gate, an inversion layer is created at the insulator-semiconductor interface, resulting in a conducting channel connecting the source and drain terminals. The current flowing between the drain and source electrodes can be modulated by varying the gate voltage. Part of the MISFET family is the MOSFET (metal-oxide-semiconductor FET) which is built on the CMOS technology, and is what most of the semiconductor industry is about.

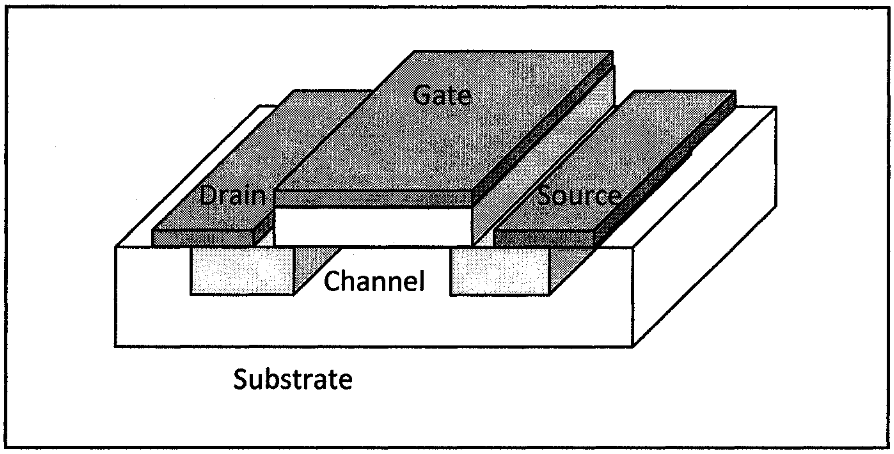

Figure 2-5. MISFET Structure

Another FET device structure of interest is the thin-film transistor (TFT). TFTs, first described by Weimer in 1962 [24], are more suitable for large area applications where it is hard to obtain single crystal cuts of such dimensions. Materials used for such structures are polycrystalline and amorphous silicon, which are deposited as thin films. Organic semiconductors can also be deposited as thin films by using various coating techniques and evaporation. Although charge carrier mobility is lower for inorganic TFTs due to the non-single crystalline active regions, there are applications were their performance is quite sufficient. Also, instead of operating in the inversion regime, TFTs operate in accumulation mode.

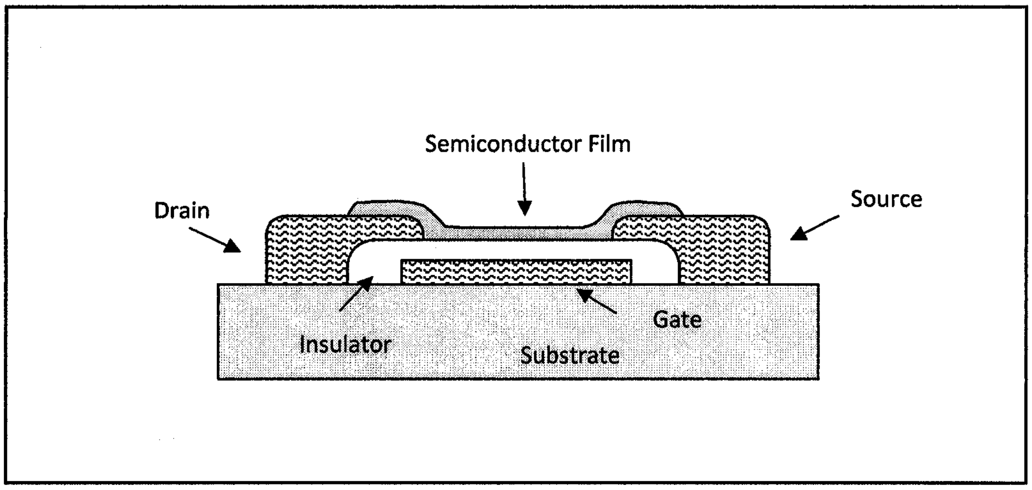

Figure 2-6. Thin Film Transistor (TFT) Structure.

Several device configurations are available for the fabrication of OFETs. Figure 2-7 shows the most commonly used structures: top-contact, bottom-gate; bottom-contact, bottom-gate; and bottom-contact, top-gate.

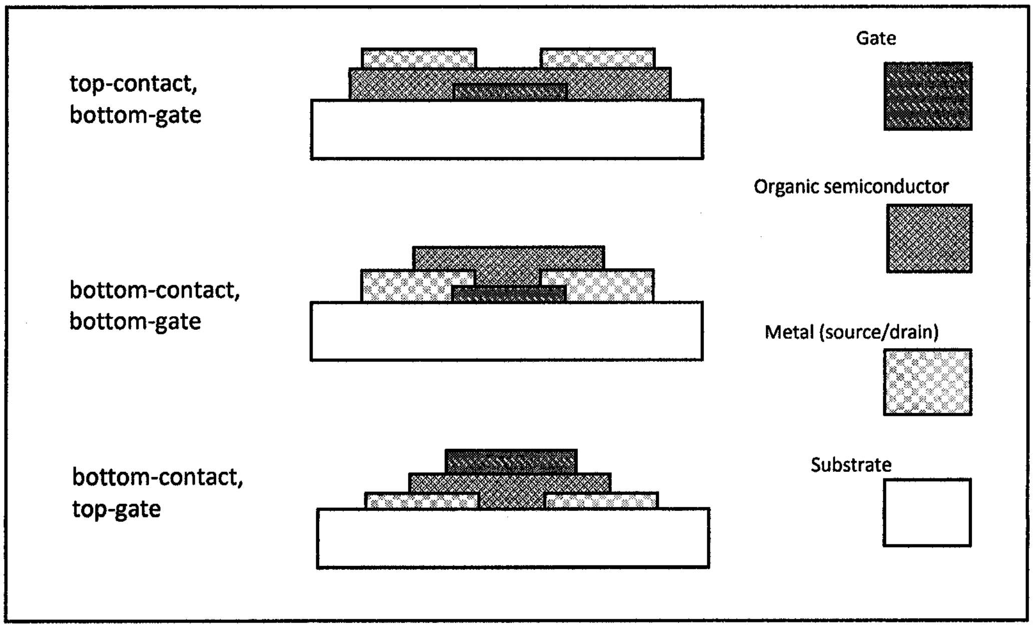

Figure 2-7. Cross-section of commonly used OFET structures.

Both organic small molecules and polymers can be used to fabricate OFETs. As mentioned earlier, small molecules offer higher performance at a higher processing cost, through vacuum deposition. Organic polymers are most often spin casted, drop casted, dip coated; or selectively deposited through direct printing. However, their mobility trails about one order of magnitude behind small molecules. Thus, in order to improve performance of organic polymer devices, extensive microstructure characterization has been done on polymer thin-films. Given that the highest mobilities are obtained by SCO OFETs, structural order of polymer chains holds the key for improving its performance.

3 Pattering Techniques for Organic Semiconductor

3.1 Soft Lithography

For several decades, optical photolithography has been the patterning technique of choice for large area and mass production applications. This lithographic technology is a relatively simple process that creates very high resolution patterns reliably at a moderate price cost. Thanks to continuous improvements of this technology, the semiconductor industry was allowed to prosper at a phenomenal rate and even keep up with Moore's Law. Moore's Law, an observation, stated that the number of transistors on an integrated circuit for minimum component cost would double every two years. Thus, photolithographic technology enabled the reduction of the overall cost of fabrication, while improving device performance over several decades.

More recently, organic polymer semiconducting materials have found their way into the microelectronics industry. Low-cost and high efficiency are the main application targets for these new materials. Polymers are typically applied over large areas by spin coating or dip coating. These material deposition methods are of very low cost; however, in order to obtain functional integrated circuits, being able to pattern polymers and isolate individual devices is a must. The successful fabrication of functional all-polymer integrated circuit devices would be the ultimate goal leading to the production of truly low-cost and disposable electronics.

Given the success of optical photolithography in the domain of inorganic semiconductors, it is natural to be inclined towards adapting this technology to use with organic materials. However, this process is not suitable for patterning organic materials directly for a number of reasons. Sub-micron photolithography degrades active polymers due to solvents used and sometimes, their complexity increases the costs of fabrication so much that it defeats the low-cost target of polymer devices. In order to remain in the realm of low-cost manufacturing, soft lithography family of patterning techniques were developed to tackle the difficulties associated to the printing of well defined organic material structures with ease and simplicity. Soft lithography includes techniques such as microcontact printing (μCP), microtransfer molding (μTM), micromolding in capillaries (MIMIC), replica molding (REM) and solvent-assisted micromolding (SAMIM). The common key element present in this family of patterning methods, extensively researched by Whitesides' group [25], is the use of a poly(dimethylsiloxane) (PDMS) stamp, a "soft" elastomeric material. Inkjet printing of organic materials is also another promising technology in this field. Several research groups have successfully printed functional organic devices using slightly modified consumer inkjet printers and there have been reports of working display panels fabricated with inkjet printing.

3.1.1 Poly(dimethylsiloxane) (PDMS)

Soft lithography are techniques that make use of a "soft" rubber to shape, mold or pattern desired materials on a substrate. Several rubber materials have been used by research groups to carry out their experiments. These materials include polyurethanes, polyimides, PDMS and other cross-linked resins. Poly(dimethylsiloxane) is one of the most widely used stamp or mold materials among soft lithography researchers. PDMS is a silicone rubber that is in liquid form at room temperature and can be easily converted into solid form by cross-linking. In order to create patterned relief microstructures, the elastomer precursor is poured over a mastermold, cured through heat and separated. The master can be made of Si, photoresist or any other materials on which micropatterns can be created using conventional photolithography. Given the properties of the PDMS, stamps can be reused several times without inducing noticeable structural defects and several stamps can be prepared from one master, which renders soft lithography techniques cost effective and fabrication efficient. Additionally, the elasticity of PDMS allows for patterns to be created over planar as well as non planar surfaces. More intimate contact can be made between the substrate and the protruding regions of the stamp due to its softness. However, the aspect ratio of the features on a PDMS stamp needs to be controlled carefully in order to avoid the collapsing of roofs. PDMS stamps with reinforced structures have been studied as an attempt to overcome this problem and enhance the resolution of the patterns.

3.1.2 Microcontact Printing

In Microcontact Printing (μCP), a PDMS stamp is wetted with an "ink" using either one of the several methods available (spin coating, dip coating, etc.) and put in conformal contact with the desired substrate. Raised features of the stamp come into contact with the substrate, and when they are released, a thin layer of the "inked" material becomes printed on the surface of the substrate. Features ranging from less than one micron to several hundred microns can be printed with relatively ease and good reproducibility. This is a promising technique that can be adapted to a roll-to-roll process in the future for mass production capabilities.

3.1.2.1 Self-Assembled Monolayers

As the name implies, self-assembled monolayers are molecules that self-align in an ordered fashion to form an ultra thin film. SAMs have amphiphilic molecular structures. Amphiphilicity refers to compounds that have a water-soluble, hydrophilic, group attached to another water-insoluble, hydrophobic, group. Because of this property, such molecules can spontaneously "self-assemble" into an orderly structured array when chemically bound to a specific type of surface; thus forming a monolayer. These structures are very interesting for the fact that they can modify surface properties easily, either physically or chemically. Properties such as wetting, conductivity, adhesion and chemical reactivity can be modified at will.

Two factors determine how well SAM structures are formed. Firstly, the nature of the chemical interaction between the surface of the substrate and the adsorbate controls the "binding" of the molecules to the surface. Typical surface "binding" can occur through physiosorption (eg. Van der Waals forces) or chemisorption (eg. Hydrogen bonding, ion pairing and covalent bonding). The latter is the most desirable to obtain stronger bonds. Secondly, the type and strength of the intermolecular interaction between the adjacent adsorbates of individual molecules plays a major role in holding the assembly together.

SAM systems of particular interests are the assembly of trialkyl-,trichloro-, or trialkoxysilanes bound to silicon dioxide surfaces, and *n*-alkanethiols to gold surfaces. These can be used as resists for wet etching [25].

Systems of *n*-alkanethiols with bounds to transition metal (eg. gold, silver and copper) surfaces has been extensively studied because it is one of the most stable and easily achieved SAM structures [26-29].

3.1.2.2 Microcontact Printing of SAMs

Pattered SAM layers are deposited on surfaces with a PDMS stamp and have mainly two functionalities: (a) they can be used as ultra thin resist layers for selective wet etching and patterning various materials depending on the type of SAM; (b) it can also modify surface properties (chemical or physical), which can be useful in certain applications. Because SAM systems of hexadecanethiols and gold are understood the most, μCP of SAMs on Au will be discussed.

Typically, the molded PDMS stamp with relief structures is wetted with a solution of hexadecanethiol in ethanol (~2 mM). Then it is brought in contact with a substrate evaporated with a thin layer (10-200 nm) of Au. The Hexadecanathiol ($CH_3(CH_2)_{15}SH$) forms patterns of hexadecanethiolate ($CH_3(CH_2)_{15}S^-$) on gold upon contact. It does not take long for alkanethiolates to form on gold; usually, within seconds a highly ordered SAMs layer is formed for a microcontact printing process. Whitesides group have developed three different μCP configurations for printing SAMs (Figure 3-1). Figure 3-1a illustrates the most common approach for printing on planar surfaces with a planar stamp. In Figure 3-1b, a rolling stamp is used for printing on a planar surface; and finally Figure 3-1c, a non planar surface is being printed by a planar stamp by rolling the surface on it.

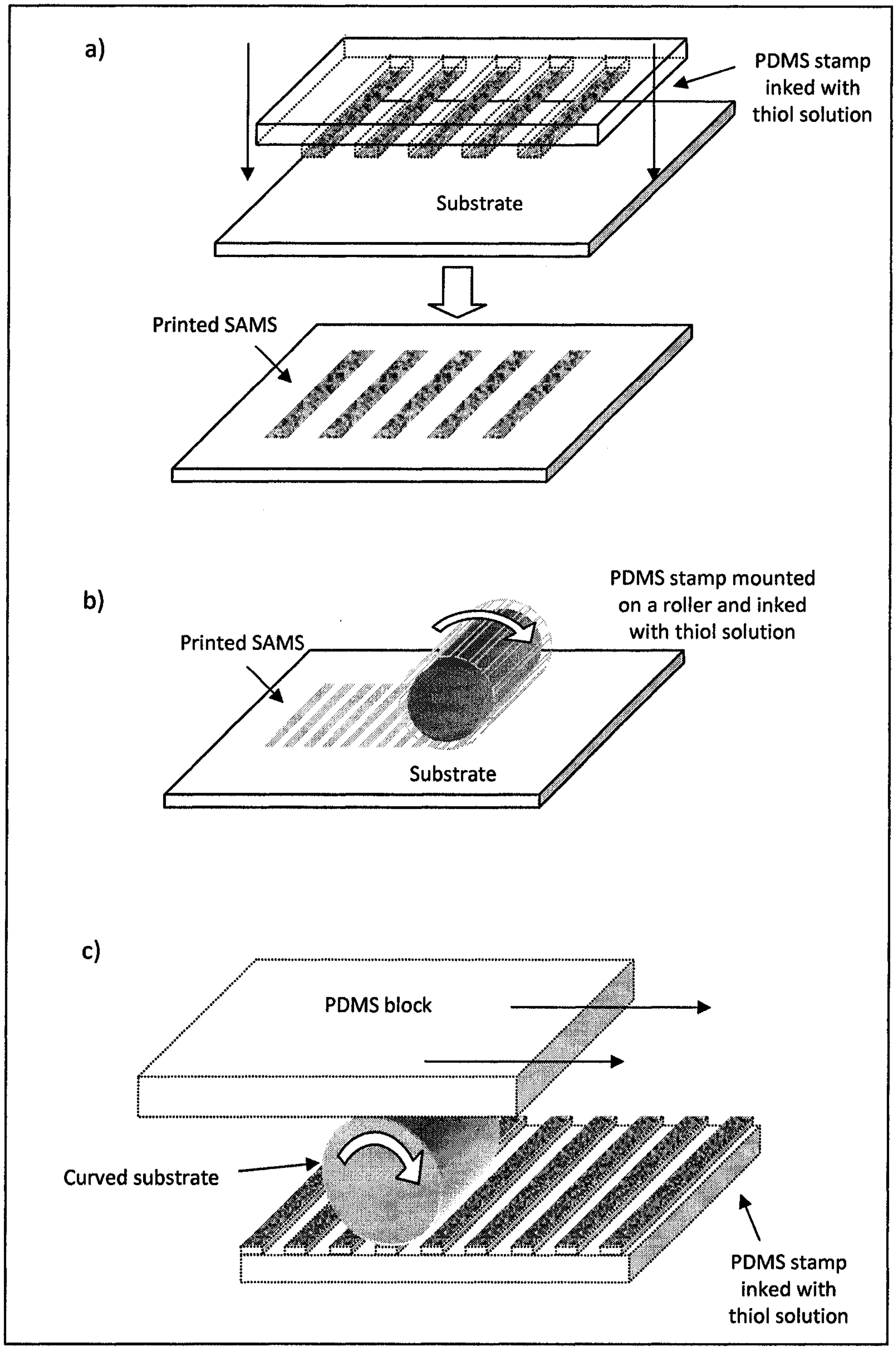

Figure 3-1. Microcontact Printing of hexadecanethiol on gold surface.

3.1.2.3 Microcontact Printing of Polymers

Microcontact printing was originally developed for, but not limited to, the use of printing self-assembled monolayers (SAMs). Polymer inking and stamping was demonstrated by Li *et al* [30] where functional organic TFTs were fabricated with patterned poly(3,4-ethylenedioxythiophene)/poly(4-styrenesulphonate) (PEDOT) as source and drain electrodes. Field-effect mobilities obtained were as large as 0.7 cm^2/Vs and on/off current ratios in the order of 10^6. Patterning of PEDOT by µCP has also been reported by Granlund *et al* [31]. In their publication, they described the fabrication of several arrays of passively addressed polymer light-emitting diodes (PLEDs). The substrates used were glass coated with a thin layer of Au or ITO. Stripe lines of PEDOT of 100 µm in width were printed onto the substrates using a PDMS stamp with relief patterns (Figure 3-2). The basic stacked structure of the PLED comprises of a light-emitting polymer material (red-emitting poly(3-(2-butyloxy-5-octyphenyl)thiophene (PBOPT)) sandwiched between a cathode (Al) and an anode (Au or ITO). A layer of PEDOT is placed between the anode and the active polymer to increase the carrier injection. Interestingly, Granlund *et al* used the printed layer of PEDOT as etch resist for substrates coated with Au, for isolating the PLED stripes. However, for ITO substrates, PEDOT could not be used as resists for etching the ITO; nevertheless, electroluminescence could only be observed in regions where PEDOT was present. This is most likely due to better carrier injection in those areas.

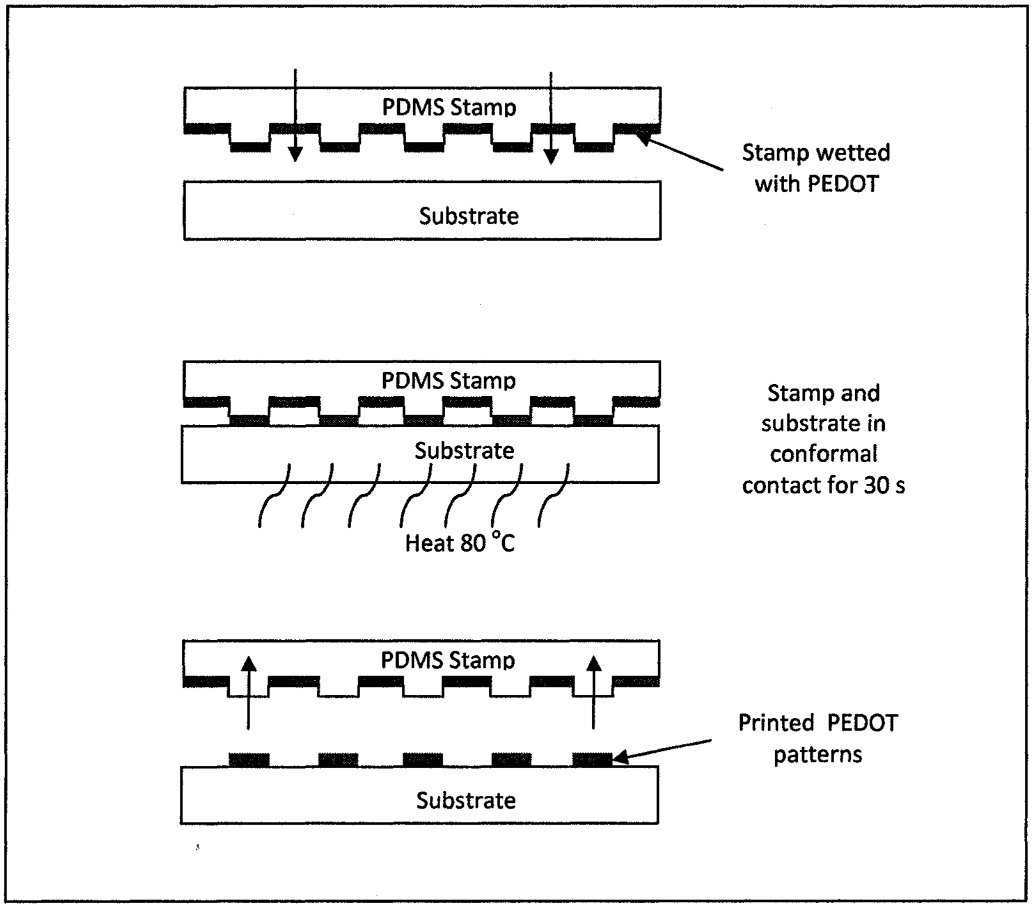

Figure 3-2. Microcontact Printing of PEDOT polymer

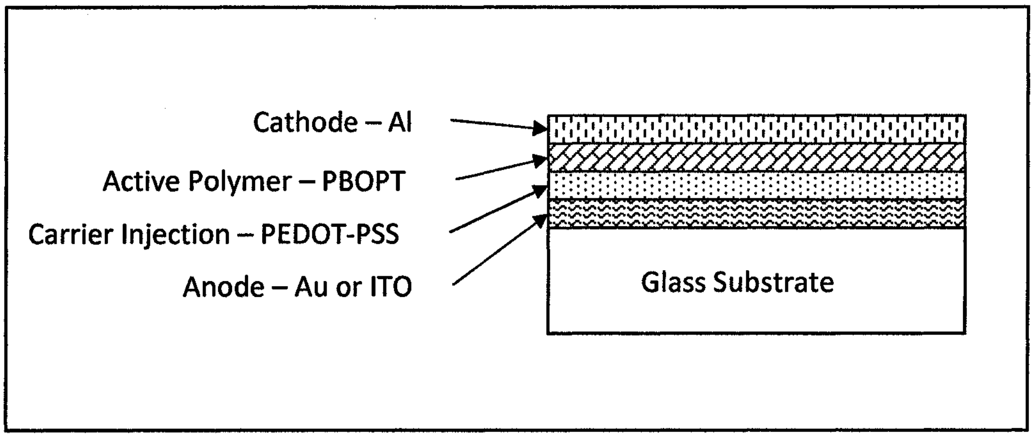

Figure 3-3. PLED Structure

3.1.3 Micromolding Techniques

3.1.3.1 Replica Molding (REM)

Replica molding is a simple and efficient method used for replicating structures on a surface. Traditionally, this technique uses a rigid mold to "shape" UV or thermally curable prepolymers. Compact discs [32, 33], microparts [34, 35], optical diffractive elements[36] and other plastics products are often mass-produced by such technique.

REM can be easily carried out simply by applying a curable prepolymer to a mold containing desired relief microstructures and curing it either by illuminating or by heating. The mold and the cured prepolymer are separated, and microstructured polymer shapes are obtained. Whitesides' group has extended REM by using soft PDMS molds instead of rigid molds. One of the advantages claimed by using a soft mold is that it facilitates the release of smaller and more fragile structures from the mold. Furthermore, the elasticity of PDMS molds allows for the manipulation of the shapes and sizes of the final polymeric structures by mechanical approaches such as, compression, bending or stretching [25, 37, 38]. By applying a mechanical bending of the PDMS mold, features of 30 nm were fabricated with ease [37].

3.1.3.2 Microtransfer Molding (μTM)

Unlike REM, μTM does not only shape prepolymers, it actually creates patterns on a substrate. A thermally or UV curable liquid prepolymer is applied onto a PDMS mold and the excess is removed by "scraping" with a flat PDMS block or by blowing off with a stream of nitrogen. The mold filled with the desired material is then placed in contact with a substrate. The prepolymer is cured by heat or illumination and the soft mold is then peeled off carefully, leaving a patterned microstructure of the polymer on the surface of the substrate. Using the method described above, μTM usually leaves a very thin layer of about 100 nm on a flat surface between raised features. If these pattered structures are to be served as resists for subsequent etching steps, this thin film must be removed by oxygen plasma etching or reactive ion etching (RIE) [25]. Another way for filling those voids on the mold without leaving a thin layer of polymer between the raised features is to use printing to dispense the appropriate amount of liquid prepolymer into the PDMS recessed regions [39].

Microtransfer molding is capable of fabricating arrays of structures in the order of micrometers across relatively large areas (10 mm × 10 mm). Additionally, this technique allows the transfer of patterns onto non planar and flexible substrates. Many research groups have studied the feasibility of photonic band gap structures [40], optical wave guides, couplers, and interferometers [41], polymer flip chips [39], and Schottky diodes [42] using μTM techniques.

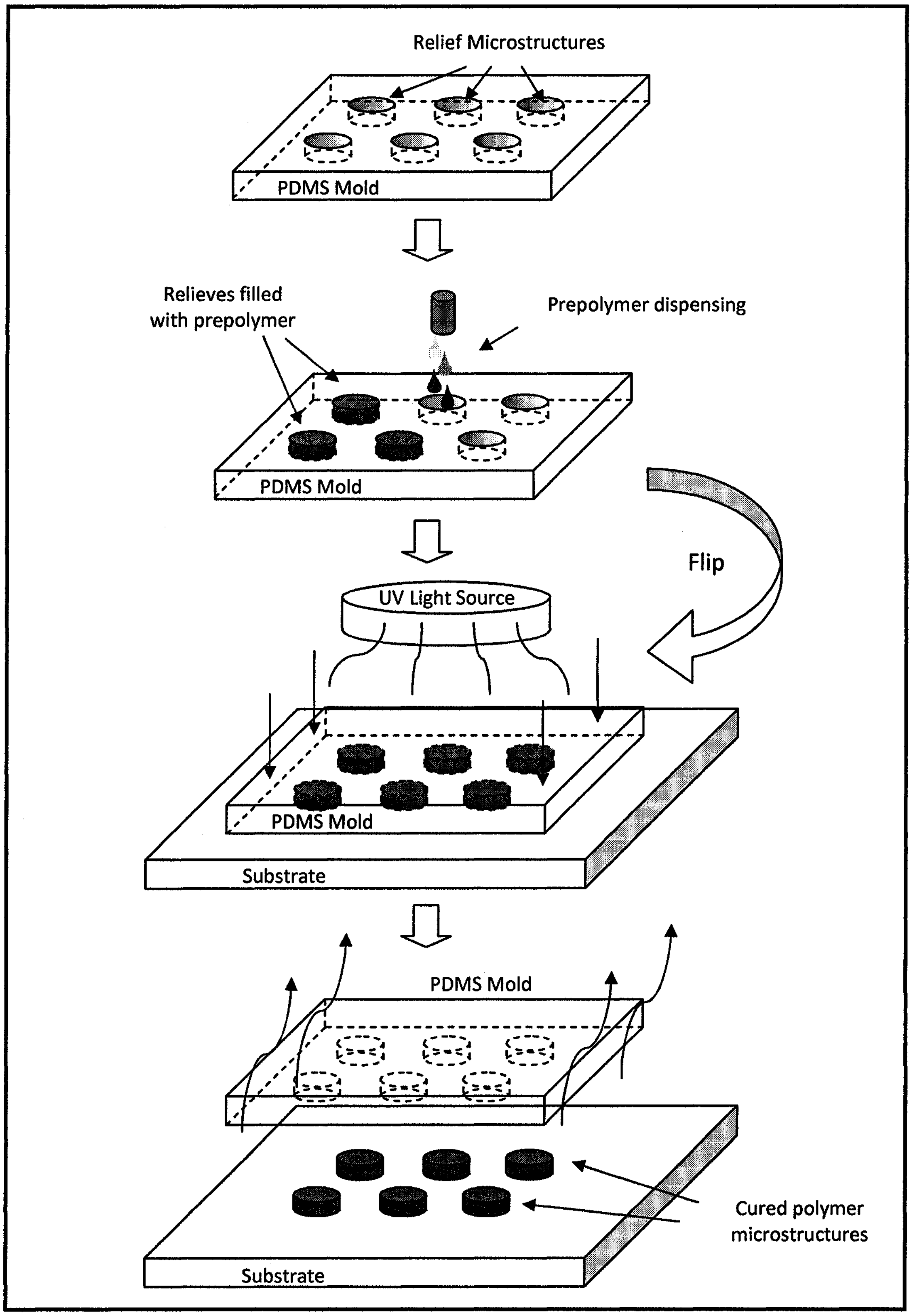

Figure 3-4. Microtransfer Molding Process

3.1.3.3 Micromolding in Capillaries (MIMIC)

MIMIC is another soft lithographic technique that makes use of a PDMS soft stamp. The bare PDMS stamp containing relief patterns is placed in conformal contact with a substrate. One of the requirements for MIMIC is that the relief patterns need to form a continuous network of capillaries. This requirement effectively limits the applicability of this technique. The empty network of capillaries is then filled with low viscosity prepolymer or any other liquid systems via capillary forces. The penetrating material is applied at one end and drawn slowly into the channels filling up the voids. The speed at which the channels are filled up is dependent on the viscosity of the penetrating material, the length of the channels and radius of the capillaries. Sometimes, a vacuum is used to help speed up the filling process.

Several research groups have demonstrated potential applications where MIMIC might be used. Jin *et al* [43] have used MIMIC to define arrays of image sensors on a curved substrate, a perfect example of soft lithography on non planar surfaces. On the other hand, Zhang *et al* [44] have fabricated conducting polymer nanowires and nanodots using the same technique on glass and Si substrates. The periodicity of the nanowires fabricated by the group was 278 nm. Blümel *et al* [45] also showed the applicability of MIMIC by fabricating source and drain electrodes of organic field-effect transistors (OTFTs) made of silver nanoparticles. The devices showed improved carrier inject into the active organic semiconductor, thus, reduction the contact effects.

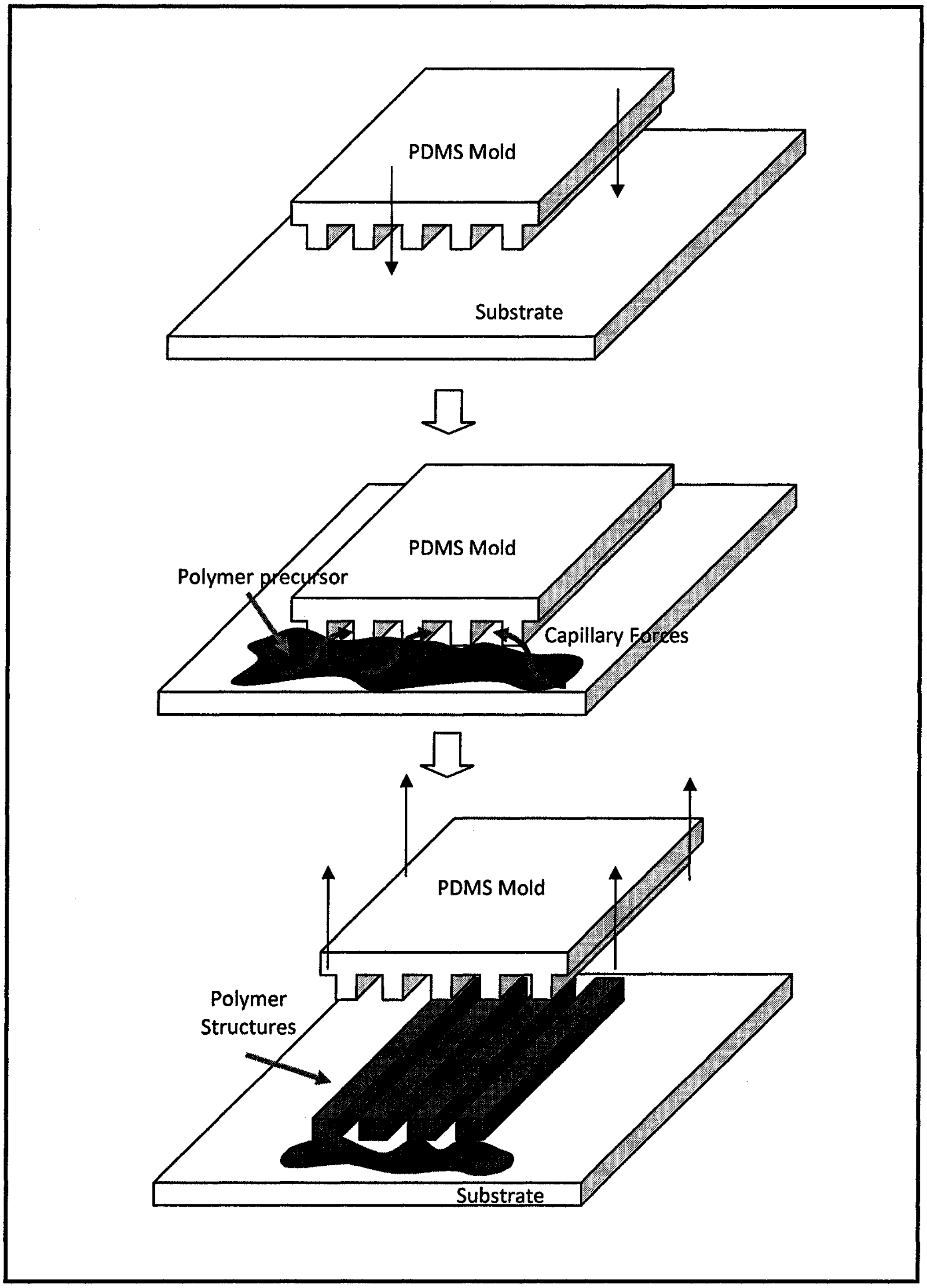

Figure 3-5. Micromolding in Capillaries Process

3.2 Inkjet Printing

Inkjet printing of organic polymers is not a lithographic technique but rather a direct writing and patterning method. Most materials which can be synthesized into a solution can be printed; even nanoparticles can be printed. Several research groups have demonstrated the possibilities of inkjet printing for various applications [46-54]. These include the fabrication of simple devices such as capacitors, polymer diodes and all-organic polymer TFTs, and more complex device circuits like high resolution organic light emitting displays (OLEDs). The only drawbacks lie in the uniformity and smoothness of the films printed, and the speed of the printing process for large area patterns. However, inkjet printing still remains as a very effective process. Only the necessary amount of material is used since patterns are created drop by drop without wasting any material. There are two classes of inkjet technology available: "continuous" and "drop-on-demand".

At first glance, inkjet printing of polymer solutions looks simple. However, many complications can arise if the solvent system is not carefully chosen. It is imperative to ensure that the inks do not interact or damage all the components inside the print head. Furthermore, the ink properties should not be modified by the mechanical shear of a piezo-electric print head or the extreme temperature conditions of a thermal print head. Besides the ink formulation, the droplet behavior once ejected from the nozzles has to be predicted with precision to ensure desired printing results are achieved.

3.3 Continuous Inkjet

Continuous inkjet technology was first developed by R. G. Sweet from Stanford University in the 1960s. Sweet showed that by applying a pressure wave pattern to an ink stream, it is possible to break it into droplets of uniform size and interval. Droplets formed are to be subjected to a charging electrode, which then pass through a deflection plate allowing the ink droplets to be either fired through or to be collected by a gutter (Figure 3-6a). Continuous inkjet technology is especially suitable for the use of ink systems based on highly volatile solvents. There are no chances of ink drying and clogging the inkjet nozzles since they are operated in a continuous mode. Additionally, the evaporation of the solvents can be compensated by adding more solvent to the ink collected by the gutter and recycling it into the system.

3.4 Drop-on-Demand Inkjet

Unlike continuous inkjet technology, drop-on-demand inkjet only ejects ink droplets when needed. Inherently, there are higher chances of having clogged nozzle using this technology. However, drop-on-demand inkjet systems are much simpler and cheaper to fabricate versus its continuous counterpart. There are two main technologies available for drop-on-demand, one uses a thermal inkjet head (Figure 3-6b), while the other uses a piezoelectric head (Figure 3-6c).

3.4.1 Thermal Inkjet

Thermal inkjet technology was originally developed by Canon in the late 1970s. The principles behind this technology are simple. Micro-chambers filled by capillary through ink channels each contain a small heating element. Electrical pulses are sent to this heater. During each pulse cycle, the ink in the area is superheated instantly to the point where a small air bubble forms. The air bubble grows and pushes the ink towards the nozzle opening up to a point where some ink separates from the orifice, forming a droplet and is purged towards the substrate. At this moment, the electrical pulse is in low, thus, no longer in the heating state. The air bubble collapses and the chamber is refilled with ink by capillary action. Thermal inkjet is limited by the type of polymers that can be used for printing. Most likely, only solutions that have a higher boiling point can be used for thermal inkjet printers. On the other hand, piezoelectric printer heads have a wide choice of materials that can be printed.

3.4.2 Piezoelectric Inkjet

Piezoelectric inkjet is the common inkjet technology in the consumer market today for graphics and arts applications. Instead of using a heating element in the print head chamber, a piezo ceramic element is used in conjunction with a diaphragm. When an electric pulse is sent to the piezo element, it induces a deformation of the diaphragm, which in turn pressurizes the chamber filled with ink and ejects a droplet. The main advantage of this print head technology is that it allows for a wider range of solvents to be used.

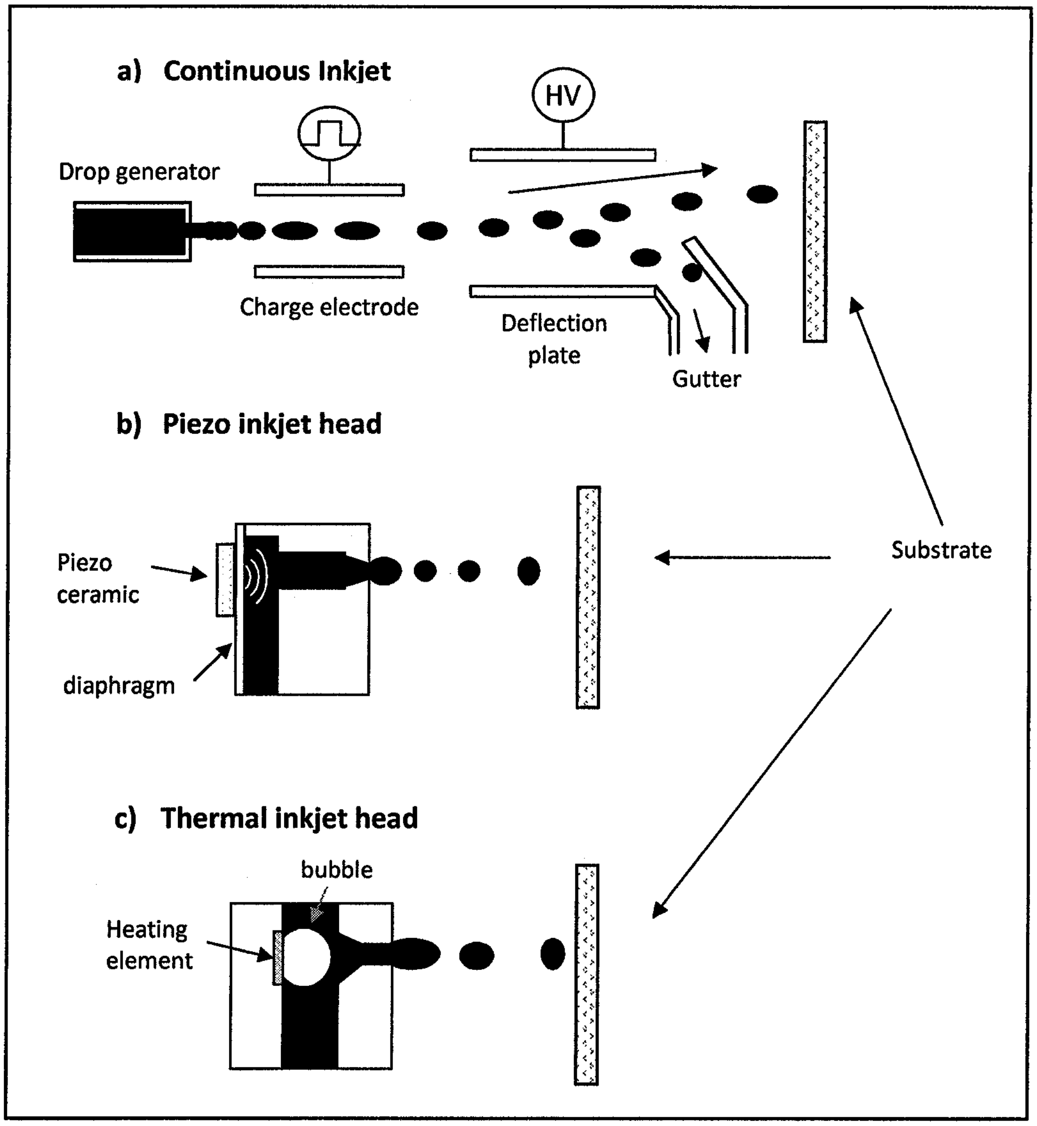

Figure 3-6. Inkjet printing technologies a) Continuous inkjet b) Piezo head c) Thermal head

4 Organic Field-Effect Transistor Fabrication

Organic thin film transistors were fabricated and characterized for this study. The organic polymer was used for the active semiconductor region was regio-regular poly(3-hexylthiophene) (RR-P3HT). A series of experiments was carried out in order to study the impact of several processing conditions on device performance. An attempt was also made to fabricate OFETs with patterned and well defined active regions with the help of a PDMS stamp. The fabrication of such devices can be described in four steps discussed in the following sections: substrate fabrication, stamp fabrication, preparation of organic polymer solution, and deposition of the active semiconductor to the substrate. The experiments were carried out in a laboratory with non-controlled environment. The ambient temperature was around 24°C with relative humidity around 35% during the whole fabrication and measurement process. Figure 4-1 shows a photograph of a sample containing several OFET devices.

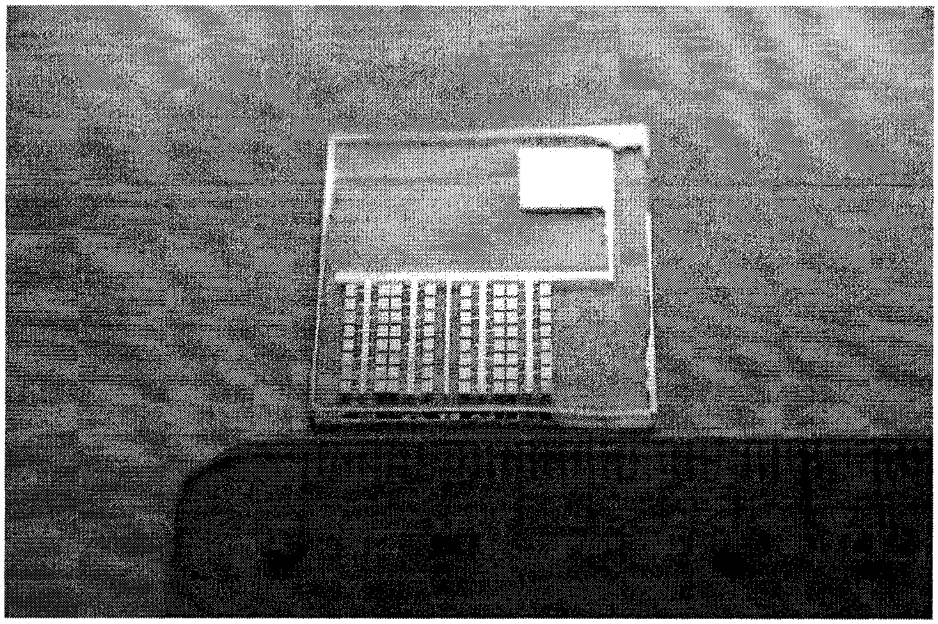

Figure 4-1. Sample containing 32 OFET devices

4.1 Fabrication of substrates

The first step towards the fabrication of OFET samples is the fabrication of the substrate. By substrate, we refer to an almost completed sample with just the last polymer deposition step remaining. The fabrication procedure for the OFET substrate includes the fabrication of the gate dielectric and the definition of source and drain metals. The TFT structure that was chosen for this experiment was the bottom contact TFT. This structure was chosen because the polymer semiconductor is only applied during the last step of the fabrication; thus reducing the risks of damage or contamination compared to a top contact for example. However, some research groups suggested that top contact OFETs offer better performance that the bottom contact counterpart.

The substrates were designed in such way that each sample could contain 16 devices. Figure 4-2 shows and overlay of the masks used for OFET fabrication. All devices have a common gate contact and 32 individual source and drain contacts.

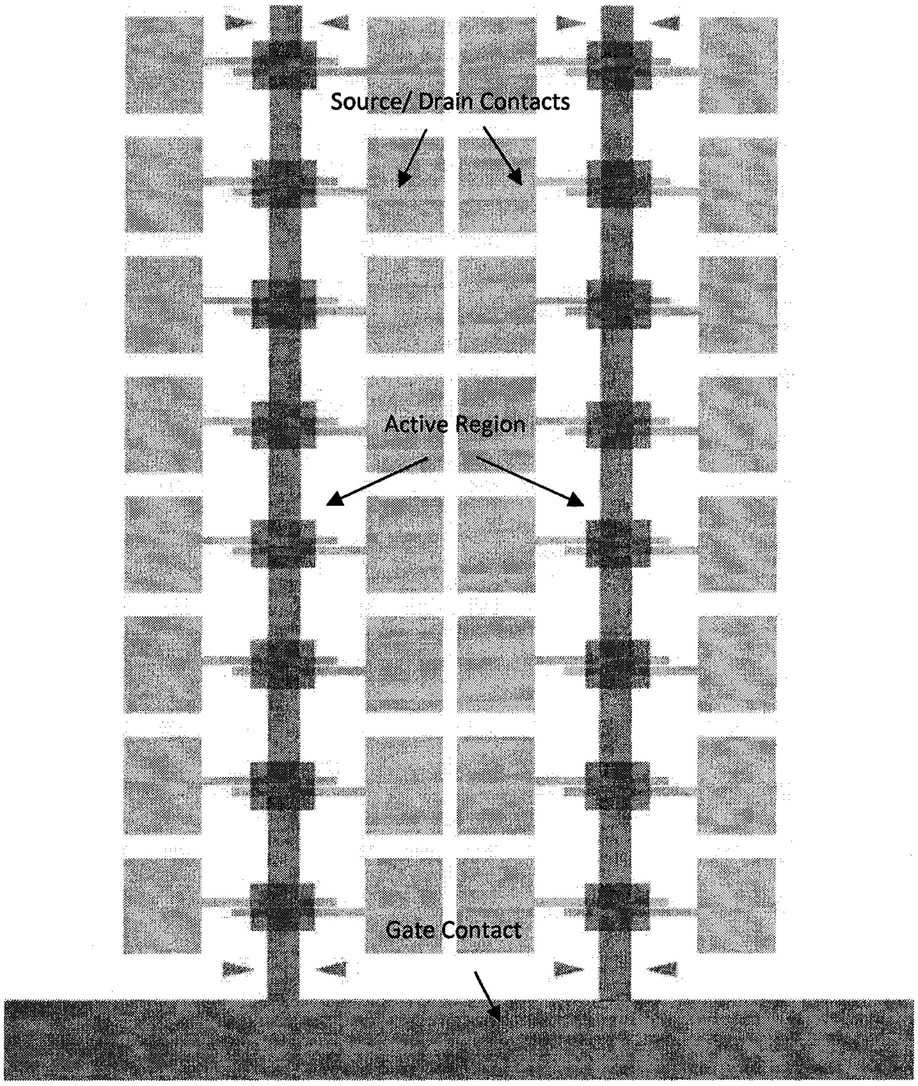

Figure 4-2. Mask layout of one OFET sample containing 16 individual devices

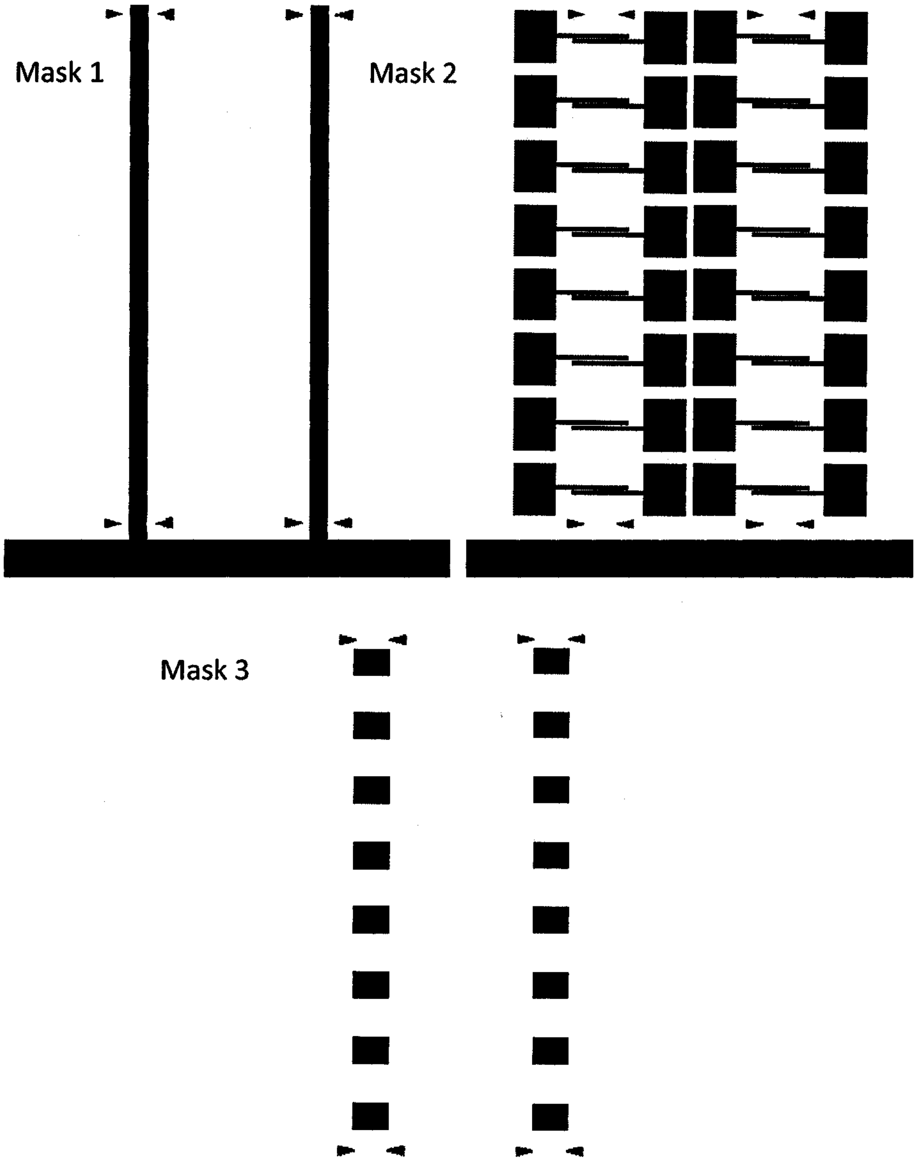

Figure 4-3. OFET fabrication individual masks

4.1.1 Gate Dielectric

All metals evaporated for this experiment were accomplished in as Edwards E306A coating system (Figure 4-5). The chosen gate dielectric for this experiment was aluminum oxide (Al_2O_3). Aluminum was evaporated on 1 mm thick glass substrates and patterned using standard photolithographic process. Shipley 1827 photoresist was then spun onto the glass substrates with evaporated aluminum, exposed and developed using mask 1 (Figure 4-3) and etched in order to define the gate electrodes. The samples were then anodized to form the aluminum oxide. The anodization procedure is relatively simple. The patterned Al samples were placed in an acid electrolyte; using the Al as the anode and another metal as the cathode (Pt), a voltage is applied between the terminals inducting a current through the Al and triggering the formation of an anodic oxide.

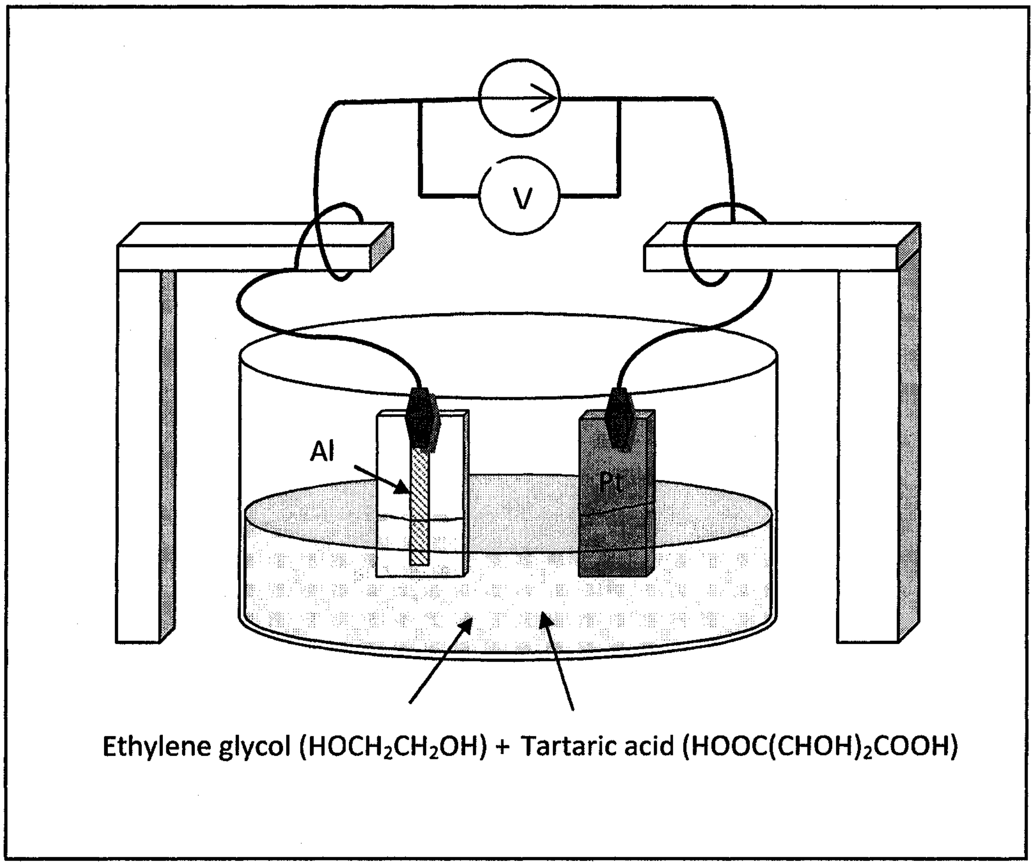

Figure 4-4. Al Anodization Setup.

Detailed gate dielectric fabrication procedure is as follow:

1) Cut Glass slides into 1x1 inch square.
2) Clean glass substrates in acetone in ultra sonic bath for 5 mins.
3) Rinse with deionized water and clean in DI water in ultra sonic bath for 5 mins.
4) Rinse and bake dry in oven at 115°C for 10 mins.
5) Load samples into vacuum chamber for Al evaporation.
6) Evacuate vacuum chamber for two hours and evaporate Al (~0.8 um).
7) Remove from vacuum chamber and spin on Shipley 1827 photoresist at 3000 rpm for 30 secs.
8) Prebake in oven for 10 mins.
9) Expose under UV lamp for 5 mins using mask 1.
10) Develop using 1:1 diluted concentrated developer and DI water.
11) Rinse in DI water 1 min and blow dry.
12) Etch aluminum using Al etchant on hot plate set to 60°C.
13) After etching, rinse with DI water for 30 secs and immerge in acetone for 3 mins to remove the photoresist.
14) Rinse with DI water and immerge in new acetone for another 5 mins.
15) Rinse with DI water and submerge DI water for 10mins.
16) Blow dry and bake in over for 10 mins at 115°C.
17) Mount samples for anodization and anodize for 1.5 hours.
18) Remove from anodization bath and submerge in glycerin for 15 mins.

19) Rinse with DI water for 1 min. And submerge in DI water for 15 mins by changing the DI water every 5 mins.
20) Blow dry and bake in over for 10 mins at 115°C.

Figure 4-4 shows the setup using for carrying out the anodization of the aluminum. The electrolyte used is an ethylene glycol ($HOCH_2CH_2OH$) solution mixed with a tartaric acid ($HOOC(CHOH)_2COOH$) and some ammonia hydroxide to bring the pH to about 7. Details of the anodization of Al procedure for gate dielectrics are be found at [55]. The thickness of (Al_2O_3) obtained for this experiment was approximately 150 nm with a capacitance per unit area of ~40 nF/cm^2.

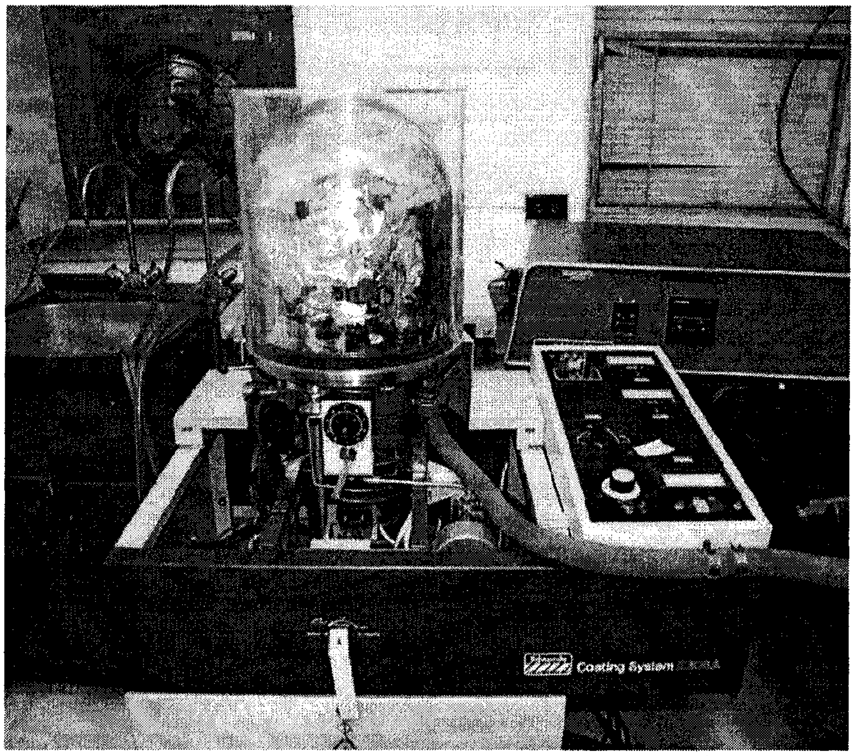

Figure 4-5. Edwards E306A Coating System.

4.1.2 Source and Drain Electrodes

The material used for the source and drain electrodes were gold (Au). Gold is known to be one of most suitable metals for making contact with organic polymers. Since most organic semiconductors are p-type, which is the case for P3HT, a high work function electrode is desirable in order to establish an ohmic contact with the semiconductor. Good ohmic contacts, also implies that the carrier injection will be efficient and not limited by a high contact resistance. The contact barrier between Au and P3HT is known to be in the order of 0.2 to 0.3 eV [56].

Mask 2 (see Figure 4-3) was used to define the source and drain metals. Patterning of the metal was carried out by a lift-off process detailed as follow:

1) Spin coat a thin layer of photoresist on substrate with gate lines prepared. (Shipley 1827 at 4000 rpm for 30 secs).
2) Prebake samples at 80°C for 5 mins.
3) Load samples in vacuum chamber for Al evaporation.
4) Evaporate a thin layer of Al (~70nm).
5) Remove samples from vacuum chamber and spin coat another layer of photoresist (Shipley 1827 at 4000 rpm for 30 secs).
6) Prebake samples at 80°C for 5 mins.
7) Expose the samples under UV light for 5 mins using mask 2.

8) Develop the photoresist with 1:1 concentrated developer diluted with DI water.
9) Wet etch the exposed Al with etchant on hot plate set to 60°C.
10) Rinse samples with DI water for 1 min and blow dry.
11) Expose samples under UV light for 5 mins.
12) Develop the exposed photo resist
13) Rinse samples with DI water for 30 secs and submerge in DI water for 3 mins.
14) Blow dry samples and bake in over at 80°C for 3 mins.
15) Load in vacuum chamber for Au evaporation.
16) Evaporate Cr to improve Au adhesion, then evaporate Au.
17) Lift-off of Au by submerging in acetone for 20 mins.
18) Rinse samples with DI water for 30 secs.
19) Submerge in acetone for 10 mins.
20) Rinse samples with DI water for 30 secs and submerge in DI water for 10 mins.
21) Blow dry and bake dry in oven at 115°C for 10 mins.

The additional Al deposition/patterning step was not necessary but preferable for performing a gold lift off process. The Al layer ensures the presence of an overhang structure (Figure 4-6); thus, resulting in a discontinuous gold film after the evaporation and facilitating the lift off process. If no overhang is present, the Au film would be continuous across the pattern and no lift off would be possible.

Figure 4-7 shows a micrograph of one of the bottom-contact, bottom-gate devices fabricated for this study.

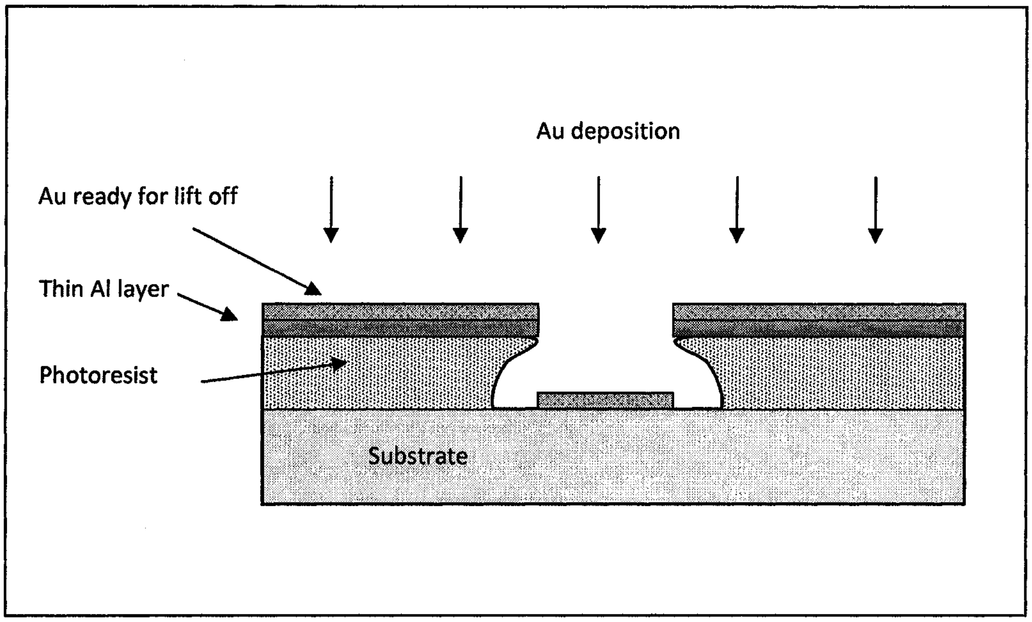

Figure 4-6. Overhang Structure for lift off process.

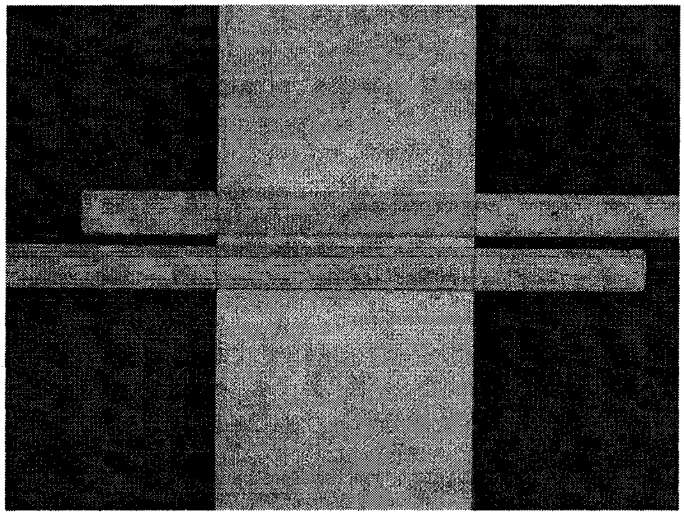

Figure 4-7. Micrograph of one of the OFET devices fabricated, ready for polymer deposition.

4.2 PDMS Stamp

In order to pattern or isolate individual devices an attempt was made to create patterns of P3HT polymer in the active regions of the devices only. According to Briseno *et al* [57], it is possible to create "islands" of hydrophilic materials on surfaces by using a "dry" PDMS stamp. This method for patterning organic semiconductors will be discussed in more detail later on.

PDMS stamp fabrication was carried out by molding and curing the silicone precursor in a patterned photoresist mold. The photoresist was patterned using conventional photolithography and coated with a release agent to prevent the elastomer from bonding to mold. The release agent used for this purpose, Fluoropel 1602, was provided by Cytonix Corporation. The PDMS elastomer, Sylgard 184, was obtained from Dow Corning as a two part, a base and a curing agent, solution. The two parts were mixed with a ratio of 10:1(base to curing agent) as per recommendations from Dow Corning and cured. The detailed procedure for stamp fabrication follows in the next section.

4.2.1 Master Mold fabrication

1) Cut and clean 1x1 inch glass substrates.
2) Spin coat Shipley 1827 photoresist at 500rpm on glass substrate.
3) Prebake at 115°C for 10 mins.
4) Expose sample to UV lamp for 10 mins.
5) Develop photoresist using concentrated developer.
6) Rinse with DI water and submerge in DI water for 2 mins.

7) Hard bake in oven for 10 mins at 120 °C and let cool.

8) Spin on release agent, Fluoropel 1602, at 1000 rpm for 20 secs.

9) Bake in over for 10 mins at 95 °C.

The resulting master mold on glass substrate can be seen in Figure 4-8.

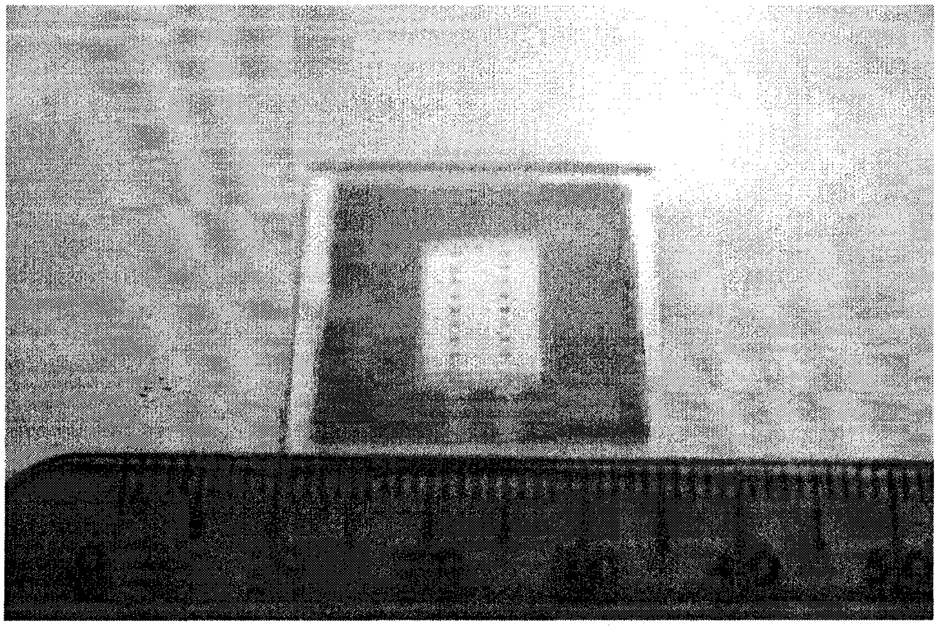

Figure 4-8. A master mold fabricated by photolithography of photoresists.

4.2.2 PDMS Stamp Molding

1) Cut and clean 1x1 inch glass substrates.

2) Make 10:1 mixture of Sylgard 184 base to curing agent in a small petridish.

3) Stir for 3 mins.

4) Let mixture sit for 10 mins until no bubbles can be seen.

5) Use pipet to put six drops of PDMS mixture on clean glass substrates.

6) Slowly put the master mold over the glass substrate with PDMS.
7) Let cure in oven for two hours at 75 °C.
8) Let sample cool and slowly separate the stamp and the master mold.

4.2.3 "Dry" Stamping of PDMS

As mentioned above, there has been a report on functional devices fabricated by patterning of P3HT and other polymers, by simply using a bare PDMS stamp. This technique makes use of selective wetting [57]. It has been reported in several publications that when PDMS comes into contact with a hydrophilic surface, it releases low molecular weight siloxane oligomers [58-60]. This may not be desirable in some cases when direct printing of organic materials is being carried out as it may contaminate the functional film. However, this technique is useful in creating high definition (in the order of 10-100um) hydrophobic patterns on hydrophilic surfaces. Stamped surfaces can then be coated with the desired polymer and areas where the PDMS stamp came into contact before will be "de-wetted", thus leaving a film on non-contacted regions only.

This process is best employed on water based polymer solutions such as PEDOT dispersion in water, where the contact angle to hydrophic surfaces is very high thus facilitating the formation of those polymeric "islands".

4.3 Polymer Solution

The semiconducting polymer that was used for the experiments was 98% regio-regular poly(3-hexylthiophene) (rr-P3HT) purchased from Aldrich chemicals (Figure 4-9). The polymer powder was used as received; no further purification process was carried out. The P3HT was dissolved in toluene 0.3% w/w concentration. It has been reported in the literature that higher boiling point solvent is preferred over low boiling point alternatives for the fabrication of P3HT devices [61]. Low boiling point solvents such as chloroform evaporate too fast, thus, limiting the time in which P3HT tried to self assemble into crystalline-like structures. Therefore, toluene was chosen for this study.

The solution was prepared on a hotplate at 60 °C and stirred at 600 rpm for two hours to help the dissolution of the polymer powder. Solutions of rr-P3HT doped with iron chloride in chloroform were also prepared with weight ratios between P3HT and $FeCl_3$ of 20:1 and 40:1. rr-P3HT films doped with iron chloride ($FeCl_3$) have been reported in the past to increase field effect mobility by two orders of magnitude [62].

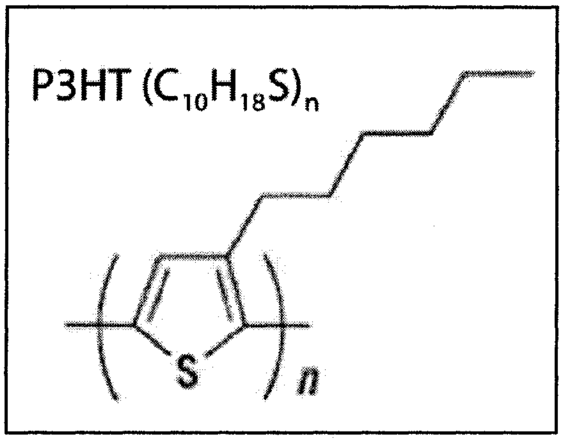

Figure 4-9. Poly(3-hexylthiophene) (P3HT).

4.4 Polymer Deposition

Organic polymer deposition is much simpler that small molecules. They can be dissolved in using organic solvents and spin coated or printed using various methods. There is no need for vacuum evaporation. The methods compared in this experiment are the spin coating and dip coating techniques. Microcontact printing was also attempted; however, no actual complete devices were fabricated.

4.4.1 Spin Coating

Spin coating of samples were performed using a Laurell WS-400B spin processor (Figure 4-10). This technique for casting polymer films on flat surfaces is one of the most popular choices. Several factors can be identified that will influence the properties of spin coated films. First, the solution needs to be able to perfectly wet the surface to be coated. Very often, the surfaces are treated through oxygen plasma or with other solvents before dispensing the desired material. Second, the final thickness of the film is determined by the acceleration final spin rate and the viscosity of the substance being used. Furthermore, the vapor pressure or evaporation rate of the solvents used in the solutions will also influence the final thickness. For very volatile solvents, if the ambient vapor pressure is not controlled, the final films will not be uniform; and some "spin-off" patterns will be visible in the resulting film. Figure 4-11 is a micrograph of an OFET substrate spun-on with P3HT in chloroform. Chloroform has a very low vapor pressure, thus, as it can be seen, the resulting film is not very uniform and the "spin-off" pattern are clearly visible. In the ideal case, the spin coating chamber should be sealed; and the spin coating should be performed in a controlled environment at a higher pressure when volatile solvents are used. The spin coating procedure in this study was accomplished in an environment with no pressure control, and the speeds used were 1500 rpm and 500 rpm. The films showed no signs of "spin-off" pattern however; this is most likely because toluene was used instead of chloroform, which have boiling points of 110.6°C and 61.2 °C respectively.

It is well known that organic materials are very sensitive to the environment at which they are exposed to; particularly in an oxygen rich environment. In the case of P3HT, oxygen can weakly bind to the polymer chains and form a charge transfer complex increasing the carrier concentration and conductivity while decreasing mobility [63]. Although, this process is reversible, it is still desirable to minimize exposure to air during the fabrication process. Therefore, during the spin coating of the samples with P3HT, care was taken to purge the spinner chamber with nitrogen before dispensing the P3HT solution.

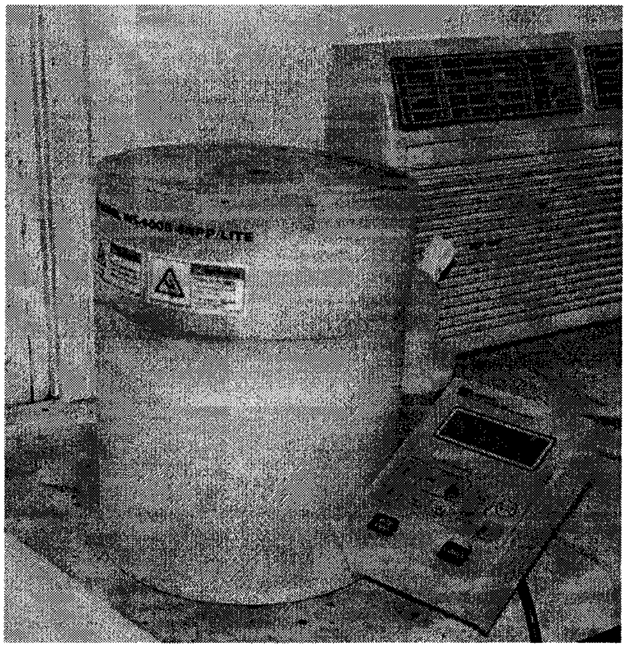

Figure 4-10. Laurell WS-400B Sping Coating System

Figure 4-11. "Spin-off" patterns on spin coated substrate (P3HT in chloroform).

4.4.2 Dip Coating

It has been demonstrated that OFETs fabricated by dip coating of P3HT polymer yield higher field-effect mobilities in general, when compared to spin coated [64-66] counter parts. Mobilities in the range of ~0.2 cm^2/Vs reported in the latter references are the highest numbers reported for P3HT to date; and those devices were fabricated through dip coating. Dip coating of those samples were carried out at a speed of 0.2-0.5 mm/s, which yielded in ultra thin-films of 20 to 40 Å in thickness [65]. This thickness translates to only two to three monolayers of the polymer. Therefore, it is possible to conclude that high mobility only requires highly ordered structures very close to the dielectric interface.

For this study, dip coating was also used for coating P3HT on OFET substrates. The coating procedure was performed in a sealed container saturated with the solvent used to prepare the P3HT solution. Figure 4-12 shows a sketch of the setup used for dip coating. The sealed nature of the dip coating chamber is necessary in order to achieve uniform drying of the film. Since the solvents used are very volatile by nature, a slight ambient gas pressure variation in the coating environment will result in a faster or slower evaporation rate of the solvent from the film, which would make a non-uniform film. Furthermore, the pulling speed of the substrate out of the solution bath was kept constant using a stepper motor puller rod controlled by computer. Two pulling speeds were used for this experiment: 0.25 mm/s and 2mm/s.

Also, the time elapsed at which the chamber is opened to remove the samples after dip coating is important. Given that it is a sealed chamber, the environment inside is filled with the vapors of the solvent; thus, the polymer film will not dry right away. This factor was also studied by letting the sample hang in the chamber after dip coating for either 20 mins or 0 mins.

Unfortunately, none of the literatures surveyed discussed in detail how their dip coating was carried out. Therefore it is not possible to verify the results obtained in this study.

One of the setbacks of the dip coating process is that usually both sides of substrates are coated with the film, which may not be desirable in some situations. Also, the substrate needs to be very clean, in order to prevent contaminations in the solution bath, which is not desirable if the same bath is to be used for multiple coatings.

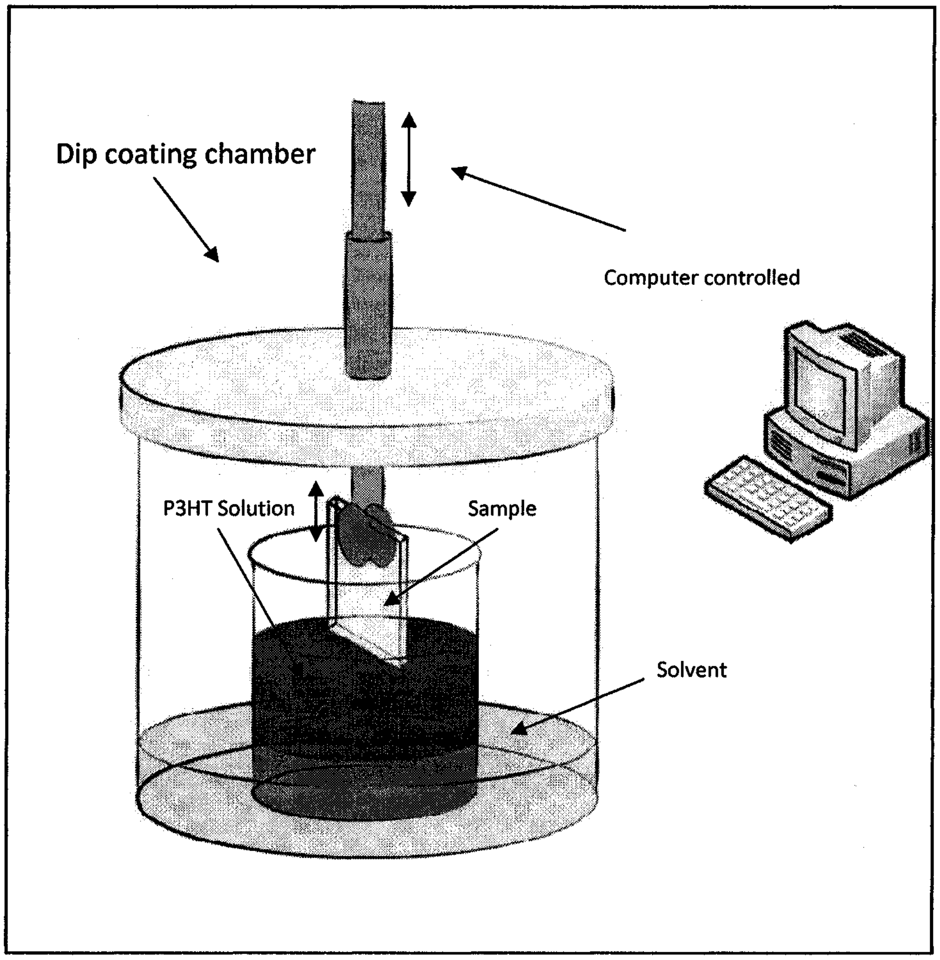

Figure 4-12. Dip coating setup.

4.5 Experimental Setup

As mentioned in the previous sections, OFETs were fabricated under different processing conditions and characterized to investigate the influence of such variations on device behavior.

All measurements of I-V transfer curves were measured using an HP 4145A parameter analyzer and a Wentworth Labs probing station (Figure 4-13).

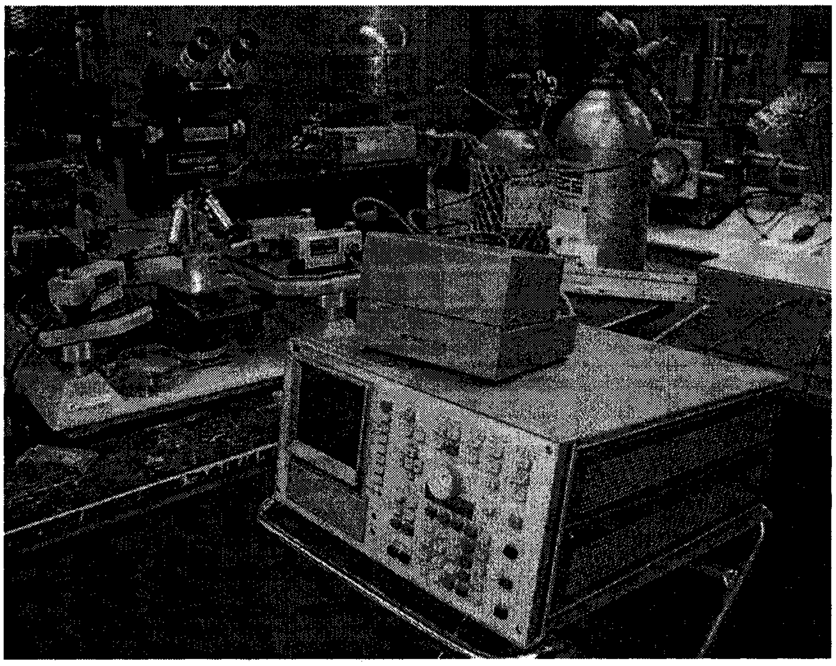

Figure 4-13. HP 4145A Semiconductor Parameter Analyzer and Wentworth Labs Probing Station.

Table 4-1 shows all the different parameter combinations for which the experiment was completed.

Table 4-1. Experiment parameters.

Samples	Experiment	Parameter	Solution	Stamping	Film Deposition	Heat Treatment (5 mins in N)	Substrate
B1, B2, B3	1a	Heat Treatment	P3HT in Toluene	no	Spin Coating (1500 rpm)	none	
						90°C	
						130°C	
						170°C	
S1	1b	Heat Treatment	P3HT in Toluene	yes	Spin Coating (1500 rpm)	none	
						120°C	
S3	2	Doping with $FeCl_3$ (P3HT:$FeCl_3$)	P3HT in Toluene	yes	Spin Coating (1500 rpm)	120°C	
S2			P3HT in Toluene (40:1)				
S4			P3HT in Toluene (20:1)				
S1	3	Substrate reuse	P3HT in Toluene	yes	Spin Coating (1500 rpm)	none	new
S5							Reused
S11	4	Dip Coating Speed	P3HT in Toluene	yes	Dip Coating (0.25 mm/s)	none	
S12					Dip Coating (2 mm/s)		
S7	5	Dip coating Wait after pulling	P3HT in Toluene	yes	Dip Coating (2 mm/s) no wait	none	
S12					Dip Coating (2 mm/s) 20 mins		

5 Results & Discussion

The results of the experiments in this chapter will be presented according to the experiment number on Table 4-1.

All the samples that were fabricated for this study had 32 OFET devices on each, where half of them (16) were stamped overnight (~12 hours) using a fresh PDMS stamp with the exception of the substrates used for experiment 1a.

The PDMS stamp had recesses structures that allowed the active regions of the devices to remain untouched as seen Figure 5-1. Fortunately, the PDMS stamp was supported by a transparent glass substrate, and PDMS itself is also transparent; both of which permitted the alignment between the stamp features and the OFET substrate with relative easy.

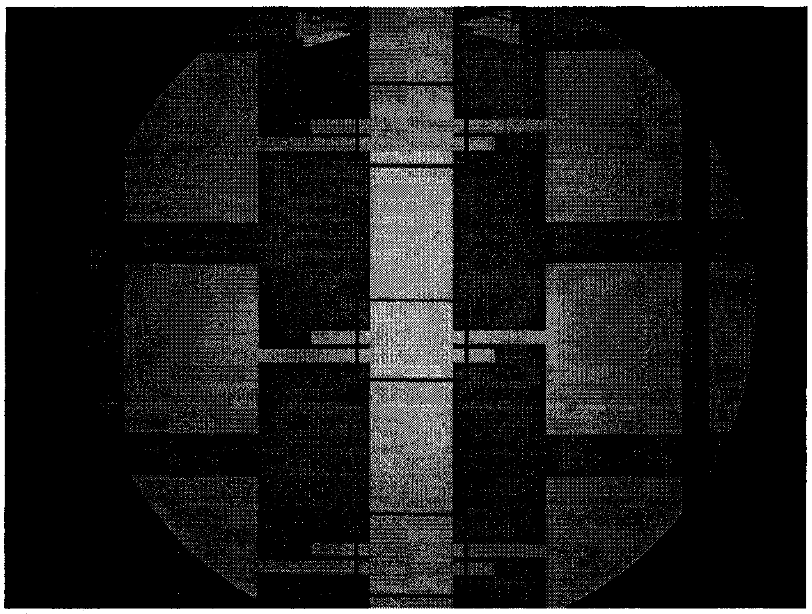

Figure 5-1. Photograph of a substrate being stamped with a "dry" PDMS stamp.

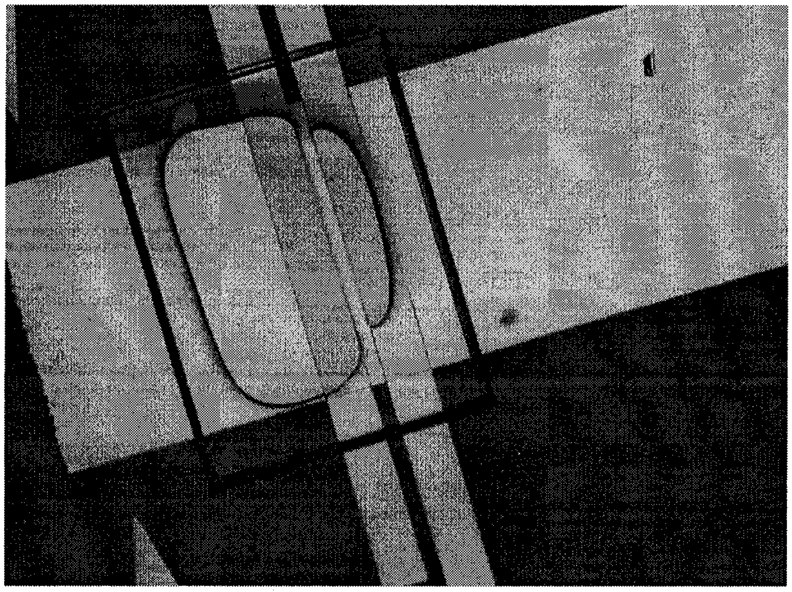

Figure 5-2. Roof collapse of PDMS recess coming into contact with the active region surface.

One of the important aspects of microcontact printing is the rigidity of the stamp material, which needs to be strong enough to prevent deformation of stamp microstructures during the printing process, as well as soft enough to promote a conformal contact between the stamp and the substrate. As it can be seen, sometimes when the "roof" of the recesses regions on the stamp are no deep enough, the PDMS material touches the active region of the FET as well.

As stated previously, prior to executing this dry stamping technique, the surface needs to be hydrophilic. In order to satisfy this condition and at the same time clean the used wafer, the bared samples were exposed to oxygen plasma for 30 seconds at the lowest power setting of a Plasma-preen II system (Figure 5-3).

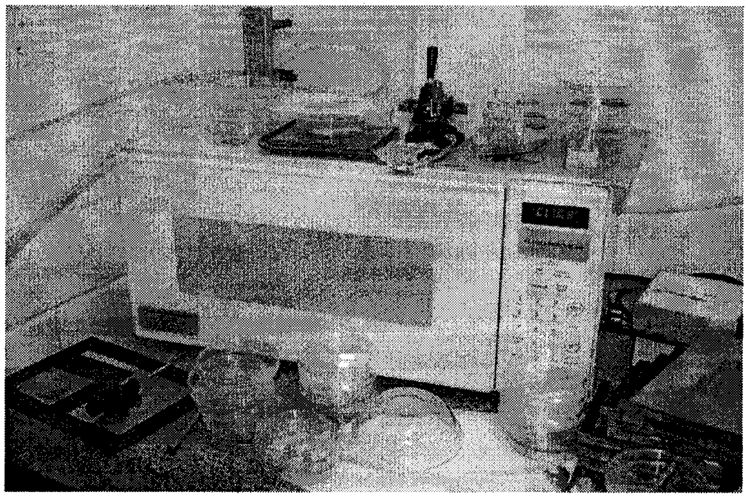

Figure 5-3. Plasma-preen II 862 plasma treatment system.

Finally, the extraction of mobility values was carried using the same method described in section 2.4.2.

5.1 Leakage Currents

The bare substrates without any polymer applied have been tested for leakage current to ensure the quality of the oxide. Figure 5-4. Gate leakage current as a function of applied gate bias.Figure 5-4 shows gate leakage current as a function of applied gate bias. Maximum gate leakage currents of a typical bare device remained in the order of 40 to 60 pA, which is quite acceptable. The leakage from gate to drain, as drain voltage is varied, is higher for a positive drain bias, suggesting a weak gate insulation in that direction (Figure 5-5). For drain to source, leakage is kept low (< 100pA) as expected from an insulating gate dielectric (Figure 5-6).

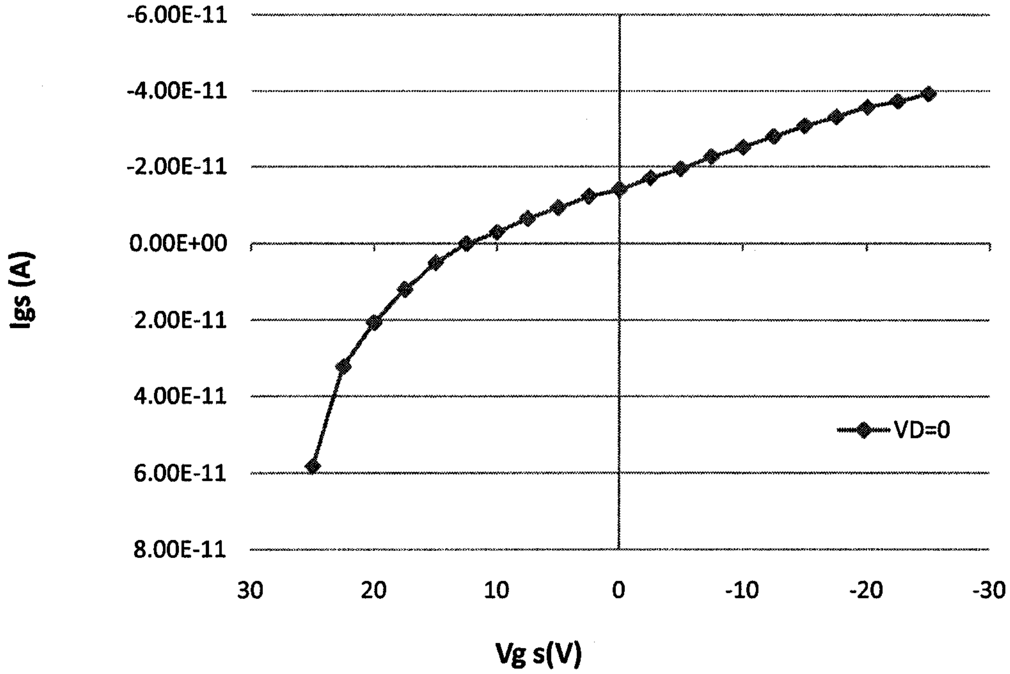

Figure 5-4. Gate leakage current as a function of applied gate bias.

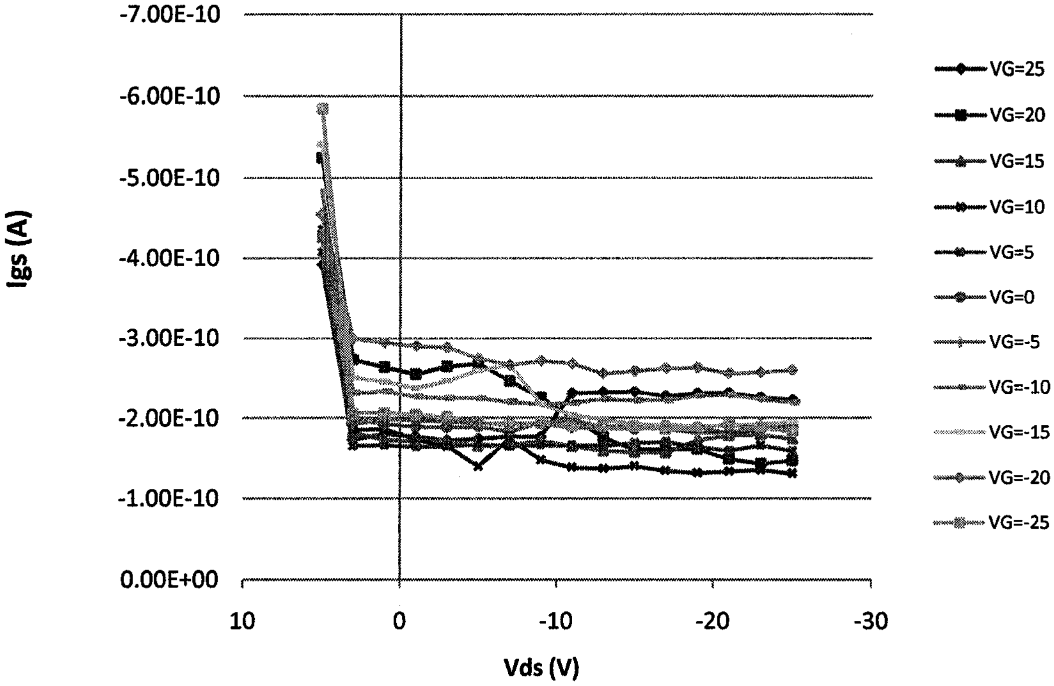

Figure 5-5. Gate leakage current as a function of drain voltage

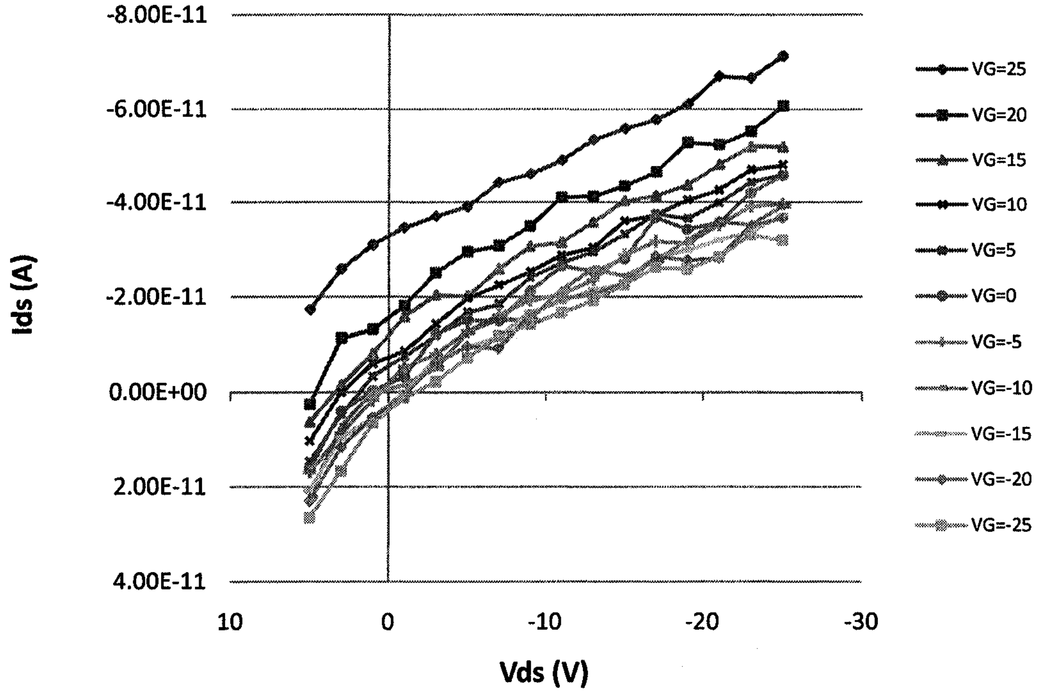

Figure 5-6. Drain current as a function of drain voltage

When polymer films are applied over the whole surface of an array of devices sharing the same gate electrode, there are inevitably maybe other paths for which current can flow. These parasitic leakages can be greatly reduced through the stamping of a "dry" PDMS stamp. Figure 5-7 and Figure 5-8 show the performance increase of stamped device versus unstamped. Since leakage current is decreased by about an order of magnitude the on/off ratio is also increased by as much.

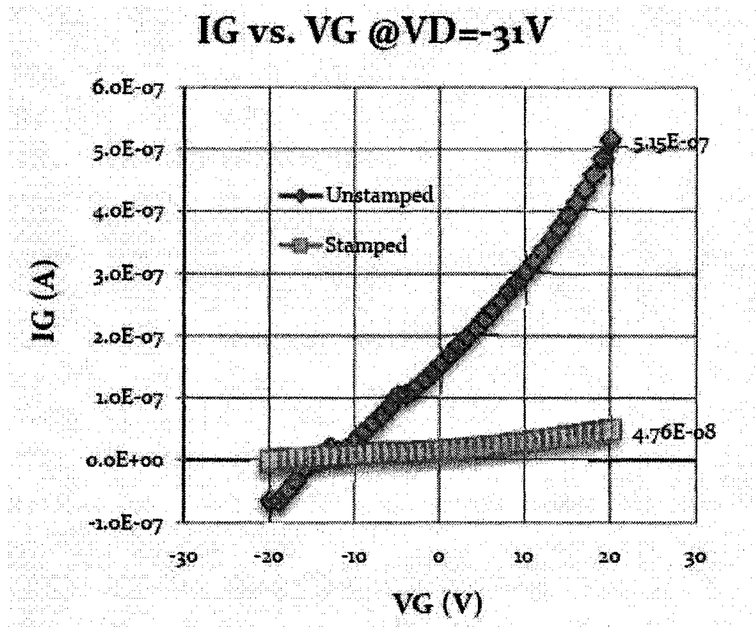

Figure 5-7. Typical gate leakage of an OFET, stamped vs. unstamped device.

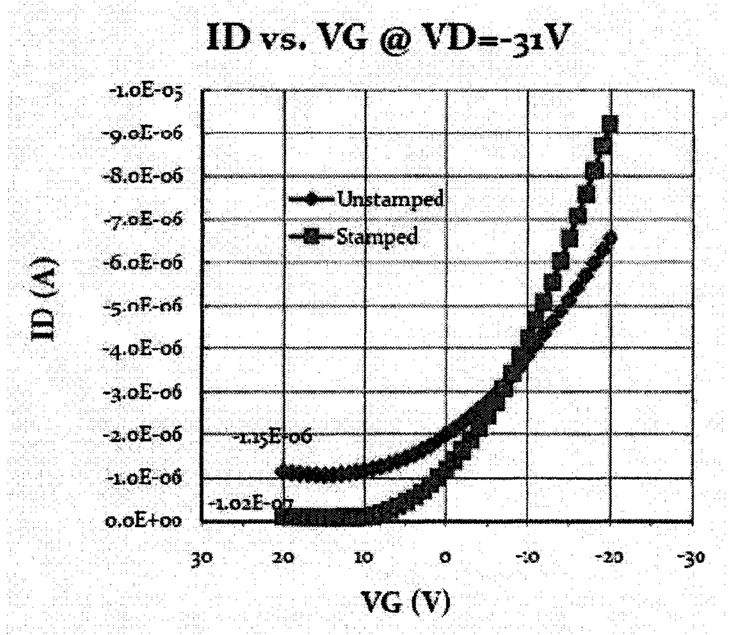

Figure 5-8. Typical ID vs. VG curve showing the difference in On/Off current of stamped vs. unstamped devices.

5.2 Heat Treatment

According to the literature, heat treatment, or annealing, of samples after deposition of P3HT as active semiconductor is important. It has been stated that thermal annealing increases the degree of crystalinity [15] and reduces the threshold voltage V_T through the partial de-doping of P3HT from residual impurities (dopant ions) [65] as well as an increase of the on/off ratio of the device.

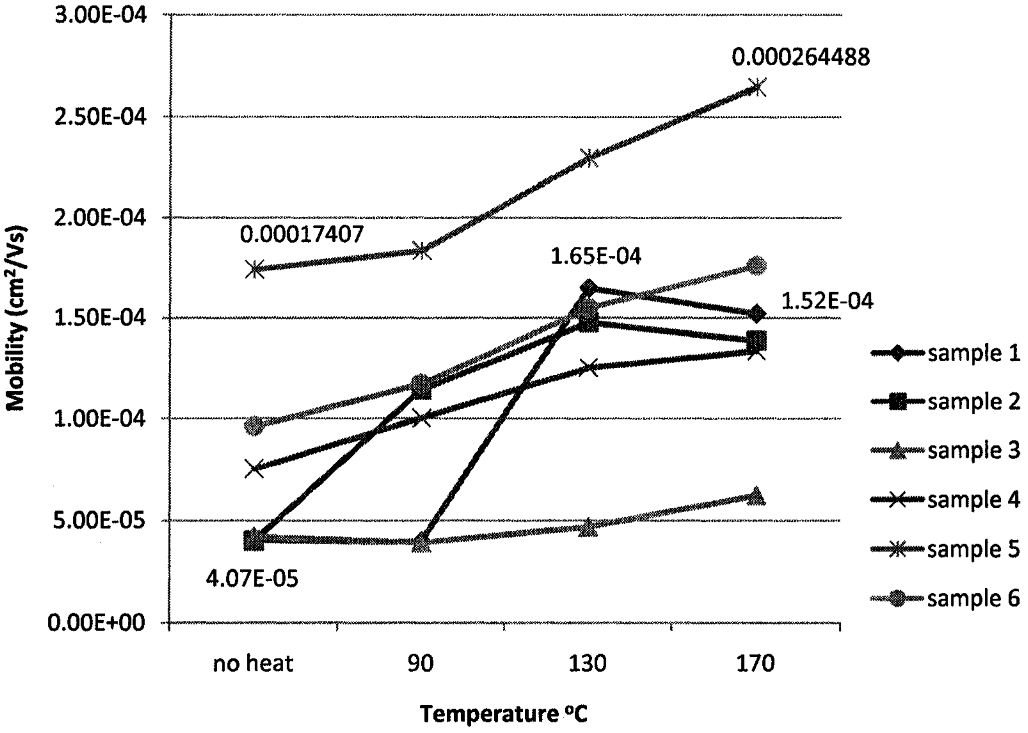

Figure 5-9. Experiment 1a, mobility vs. heat treatment temperature.

In experiment 1a, devices were fabricated by spin coating P3HT in toluene and then annealed three times: at 90°C, 130°C, and 170°C. The transfer curves were measured in between treatments. Figure 5-9 summarizes the results of six typical samples. It is clear that heat treatment increase the charge mobility in general. Taking sample 1 as an example, it can be seen that mobility increased as much as four times after annealing twice to 130°C. The differences in the increase of mobility between samples can be explained by the inherent non uniformity of the spin coating for the samples. On average, the field-effect mobility doubles after annealing compared to non treated samples. Another interesting observation is that the increase in mobility is not always positive. This implies that there exists an optimum annealing temperature and time. If treated for too long or at too high temperature, performance begins to decrease.

For Experiment 1b, the procedure was repeated as in experiment 1a; however, this time, half of the devices were stamped using a fresh "dry" PDMS stamp for 12 hours. Also, samples with annealing at 120°C (5 mins) and without annealing were compared. Table 5-1 summarizes the results for this experiment. Again, the device performance is improved after annealing the samples. But this time, the improvement is only about 30% on average. Additionally, it can also be seen that stamped devices also show higher mobility values.

Table 5-1. Comparison of mobility (cm^2/Vs) values between stamped/not stamped and annealed/not annealed samples.

Samples	Annealing	Sample 1	Sample 2	Sample 3	Sample 4	Sample 5
Unstamped	no	2.25E-05	2.92E-05	2.16E-05	2.19E-05	2.81E-05
	120°C	2.70E-05	3.63E-05	2.80E-05	2.61E-05	3.44E-05
Stamped	no	3.29E-05	3.62E-05	3.84E-05	3.68E-05	3.40E-05
	120°C	3.90E-05	4.48E-05	5.12E-05	4.58E-05	4.20E-05

5.3 Doping of P3HT with Iron Chloride

Samples fabricated using P3HT solutions doped $FeCl_3$ were measured in experiment 2. The doping ratios used were 20:1 and 40:1 (P3HT:$FeCl_3$). Devices fabricated without doping were also compared.

The field-effect mobility values extracted for non-doped, lightly doped and by heavily doped were 2.89E-03 cm^2/Vs, 2.83E-03 cm^2/Vs, and 6.48E-04 cm^2/Vs respectively. From these results, undoped and lightly doped (40:1) have roughly the same mobility; whereas, for heavily doped it decreases dramatically. The decrease in mobility can be attributed to the increase of too many charged carriers that in fact leads to a decrease in mobility as was discussed in previous chapters.

Although, lightly doping does not affect the charge mobility by a lot, the film still exhibits higher conductivity, which leaded to the inability to turn off the device (poor on/off) ratio.

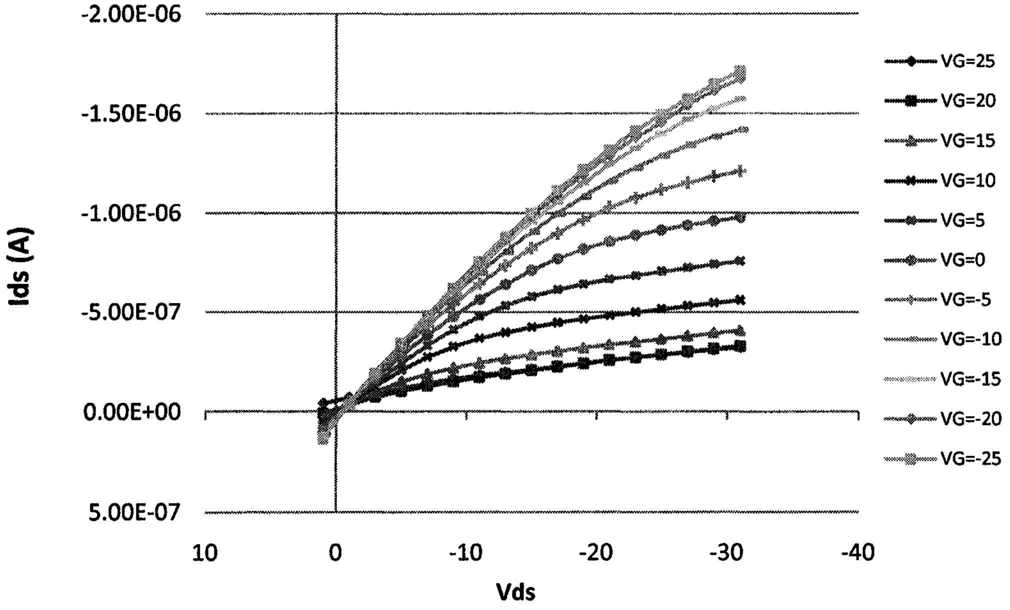

Figure 5-10. Ids vs. Vds curve of typical undoped P3HT device fabricated by spin coating.

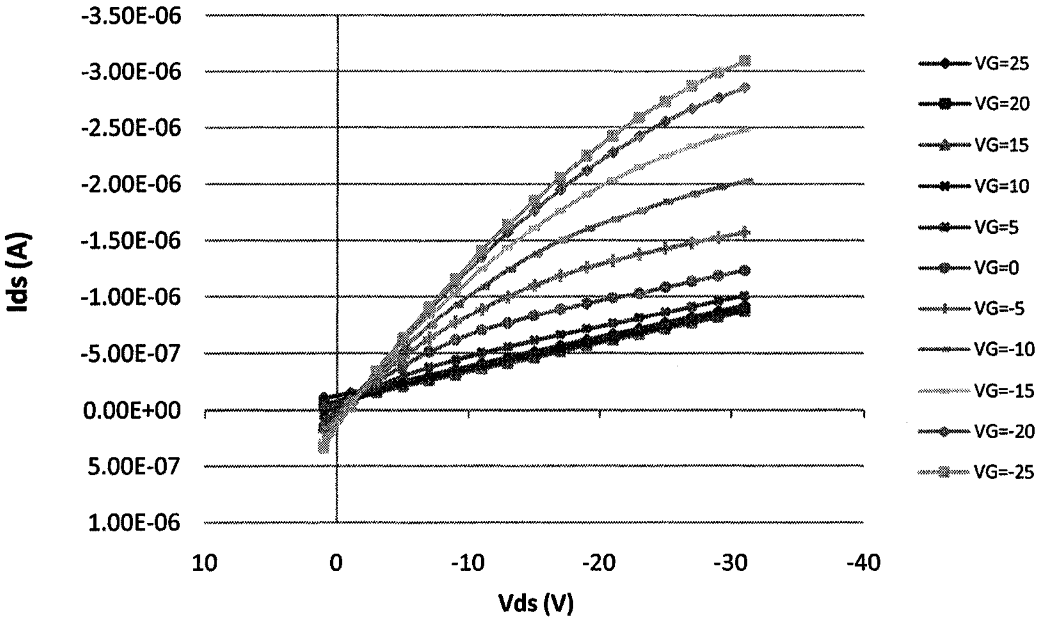

Figure 5-11. Ids vs. Vds curve of typical doped (with $FeCl_3$) P3HT device (40:1) fabricated by spin coating.

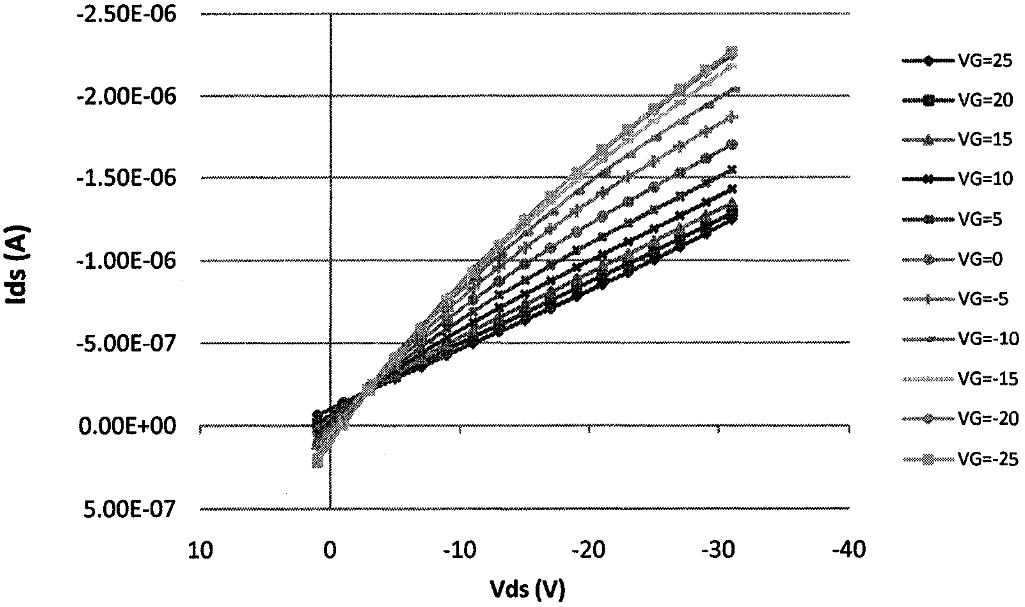

Figure 5-12. Ids vs. Vds curve of typical doped (with $FeCl_3$) P3HT device (20:1) fabricated by spin coating.

5.4 Dip Coating of P3HT OFETs

Several dip coating factors affect the final polymer film morphology and its electrical properties. Some of these factors were studied. First, the pulling speed during dip coating was investigated in experiment 4. Then, devices with two different wait times after pulling were compared in experiment 5.

Table 5-2. Different dip coating speed and stamped/unstamped devices. (Mobility cm^2/Vs).

Dip Coating Pull Speed			
0.25mm/s		2mm/s	
Stamped	**Unstamped**	**Stamped**	**Unstamped**
4.75E-03	2.50E-03	1.92E-02	7.13E-03
5.24E-03	2.82E-03	1.33E-02	8.39E-03
5.94E-03	3.67E-03	1.16E-02	6.78E-03
4.46E-03	2.85E-03	1.13E-02	6.91E-03
6.04E-03	3.30E-03	1.75E-02	7.02E-03
6.64E-03	3.63E-03	1.02E-02	7.38E-03

Results for experiment 4 are summarized in Table 5-2. A few conclusions can be draw from this experiment. First, comparing dip coating speed, devices fabricated at 2mm/s seem to offer the highest mobility recoded in the study. The highest field-effect mobility resulting from this experiment is ~0.02 cm2/Vs. Samples coated at 2mm/s versus 0.25mm/s definitely perform better at almost one order of magnitude of difference.

Also, from this experiment it is possible to see again that stamping of devices with PDMS increases the performance (the increase in mobility is close 100%).

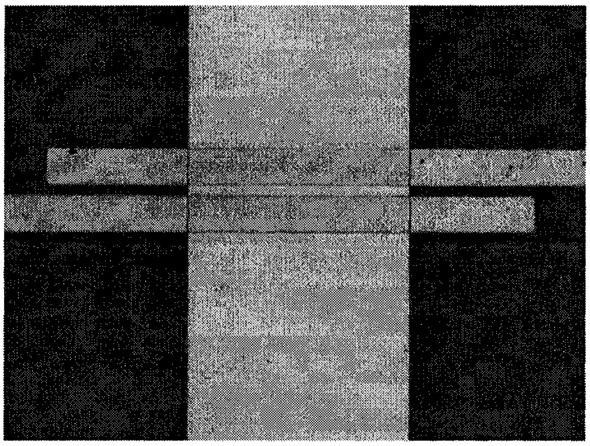

Figure 5-13. Typical S11 device (dip coated at 0.25mm/s wait 20min, stamped)

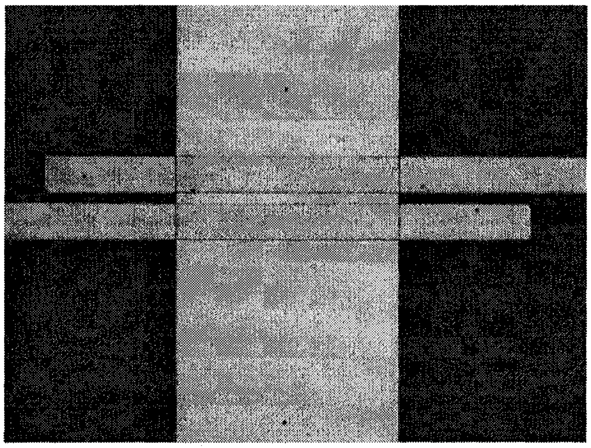

Figure 5-14. Typical S11 device (dip coated at 0.25mm/s wait 20min, unstamped)

It is interesting to note that from Figure 5-13 and Figure 5-14, not much difference can be noticed between stamped or unstamped device, except that the stamped device seems to have a little bit thicker film in the active region. The inability to create a pattern of P3HT just on the active region in this case can probably be explained by the very slow pulling speed (0.25 mm/s), which have caused the monolayer of siloxane oligomers to be washed away in the solvent.

For the devices that were pulled at a faster rate (2mm/s) Figure 5-15, a very clear definition of P3HT pattern is visible on top of the active region.

Table 5-3. Comparison of waiting time after pulling (Mobility cm^2/Vs).

No wait		**Wait of 20 mins**	
Stamped	**Unstamped**	**Stamped**	**Unstamped**
3.65E-03	1.34E-03	1.92E-02	7.13E-03
4.47E-03	2.00E-03	1.33E-02	8.39E-03
6.93E-03	1.55E-03	1.16E-02	6.78E-03
4.55E-03	1.38E-03	1.13E-02	6.91E-03
4.20E-03	1.03E-03	1.75E-02	7.02E-03

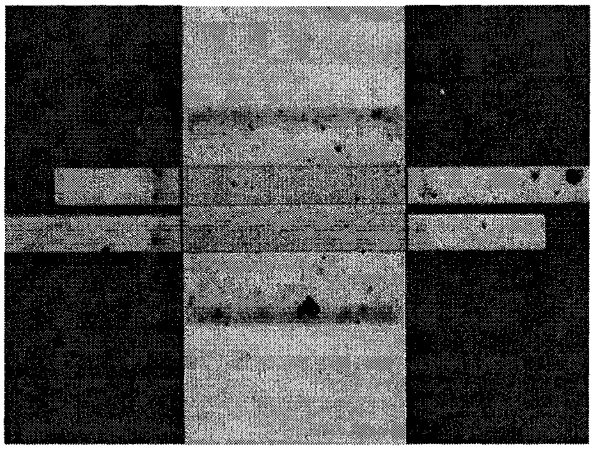

Figure 5-15. Typical S12 device (dip coated at 2mm/s wait 20min, stamped)

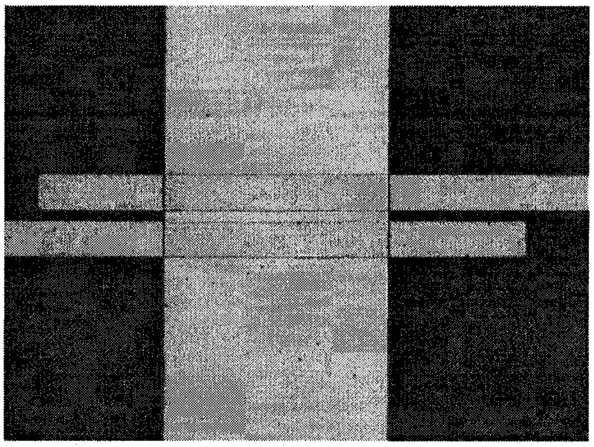

Figure 5-16. Typical S12 device (dip coated at 2mm/s wait 20min, unstamped)

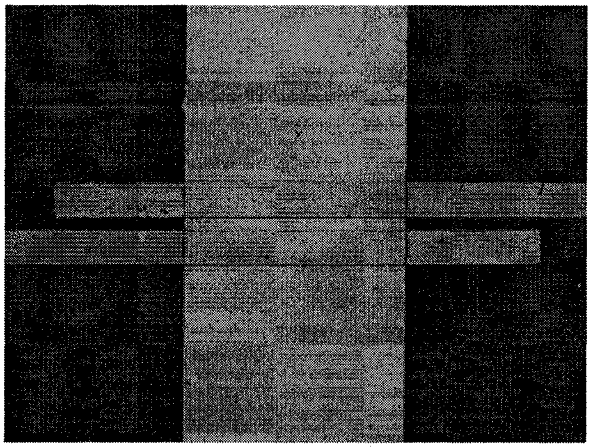

Figure 5-17. Typical S7 device (dip coated at 2mm/s, no wait, stamped)

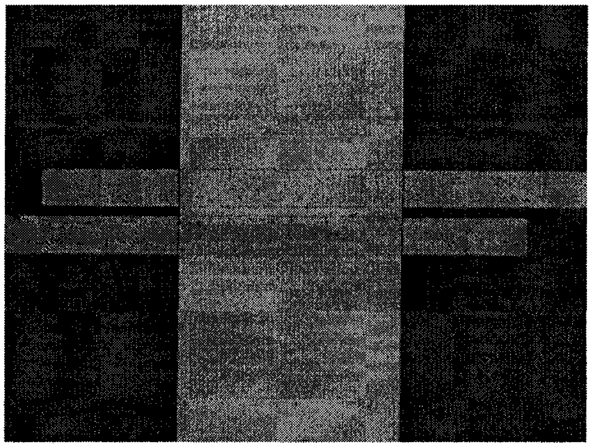

Figure 5-18. Typical S7 device (dip coated at 2mm/s, no wait, unstamped)

Comparing devices that were dip coated and removed from the chamber with waiting or without waiting time confirms that without waiting the film seems to be much thicker (darker film). From Table 5-3, it can be seen that without waiting performance is lower. This might not be caused by the thicker film, but rather, by a less crystalline structure of the P3HT. As stated earlier, P3HT polymer tends to self assemble in an ordered fashion to a certain extent after being deposited through a solution.

Another interesting observation that can be seen is that, although some stamped devices do not show a visible pattern; they still perform better than their unstamped counterparts. A possible explanation for this phenomenon is that although the surface tension is not high enough to "de-wet" the P3HT solution in toluene, it is very probable that the monolayer of siloxane oligomers is acting as an insulator and stops some of the parasitic leakage current increasing the overall performance of the OFETs. In fact, there have been reports about the possible use of PDMS as gate dielectric in some OFETs [67].

5.5 Reuse of Substrate

For spin coating, parameters that were investigated were the influence of reusing a substrate (experiment 3) and the speed of the spin coating (experiment 6).

One of the substrates that was coated in a previous experiment was reused after thoroughly cleaning with toluene and rubbing with a cotton swab. The cleaning was followed by dry baking at 90°C for 10 mins. The results showed no significant degradation in performance of the reused device. This indicated that the gate dielectric is strong enough to withstand the stressed caused by the cleaning process.

Table 5-4 shows the mobility values extracted for devices that are on a substrate that was previously used. Oddly, the results are similar for stamped and unstamped devices. The only possible explanation for this to happen is that the stamp was maybe over cured thus, became depleted of siloxane oligomers.

Table 5-4. Mobility values (cm^2/Vs for a reused sample that was spin coated at 1500 rpm

Reused Sample (spin coated at 1500rpm)	
Stamped	**Unstamped**
3.33E-03	5.31E-03
6.72E-03	3.73E-03
4.99E-03	6.68E-03
5.08E-03	6.13E-03
4.06E-03	3.55E-03
2.92E-03	3.47E-03

Looking at Figure 5-19 and Figure 5-20 concludes that in fact, there seems to be no different at all between stamped and unstamped devices.

Figure 5-19. Typical S9 device (spin coated at 1500rpm, stamped)

Figure 5-20. Typical S9 device (spin coated at 1500rpm, unstamped)

6 Conclusion and Summary

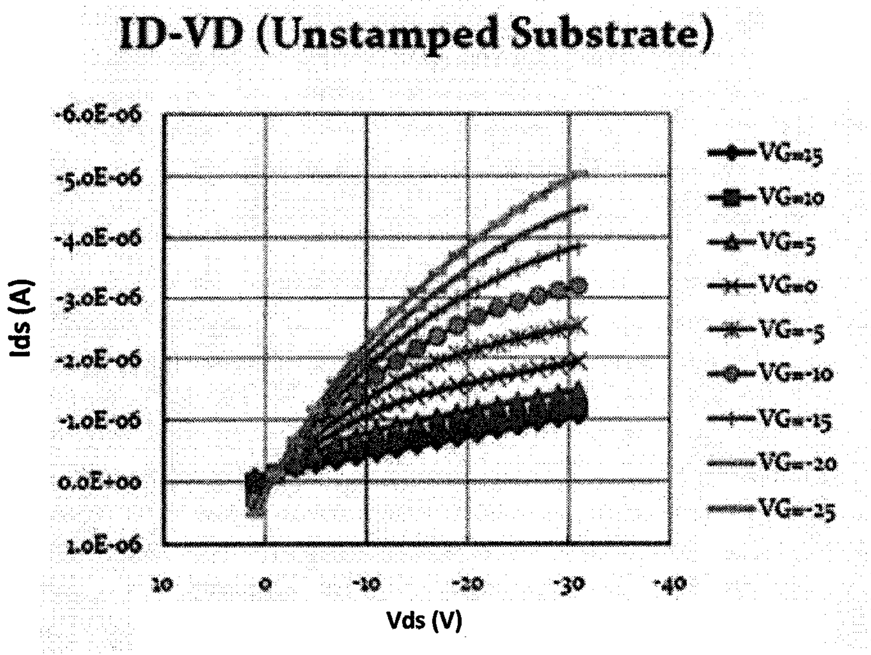

Figure 6-1. Best P3HT device IV-ID curve fabricated in this study by dip coating and dry stamping of PDMS.

In conclusion, various processing conditions of P3HT OFET devices were investigated. Results show good match with the literature. Namely, annealing of P3HT devices after deposition the active polymer generally, improves the performance (increase in carrier charge mobility). Also, dip coating deposition technique of P3HT polymer layer offer higher performance compared to spin coating techniques (Figure 6-1 and Figure 6-2). This is attributed to the increase in structural order of the polymer chains in the film and also to the improvement of the overall uniformity of the film.

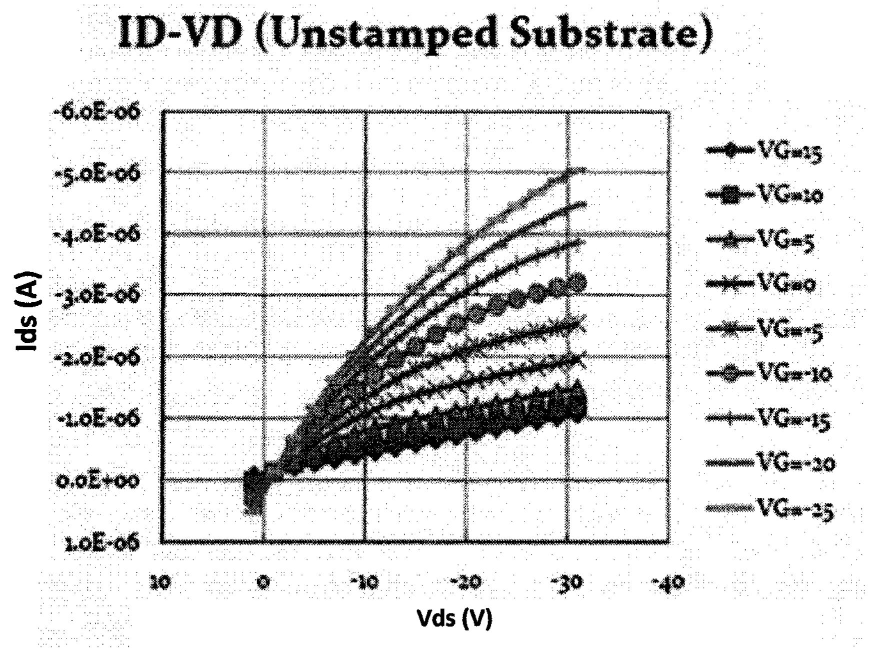

Figure 6-2. Best P3HT device IV-ID curve fabricated in this study by spin coating and unstamped.

"Dry" stamping of PDMS before deposition of the active semiconductor polymer offers improvements in device performance such as: a reduction in parasitic leakage currents across an array of P3TH OFET devices sharing the same gate electrode, an increase in charge carrier mobility of OFETs, and device isolation for devices fabricated on a same substrate through a single deposition of the organic semiconductor polymer.

6.1 Future Work

Although great progress has been made in improving organic device performance over the last few years, there is still a great deal of work to do. Organic semiconducting technology is still in its infancy and there are many questions that remain unanswered or debated. Possible directions to take for the continuation of this topic are: the use of plastic flexible substrates, the investigation on use of spin-on gate dielectrics, the use of conductive polymers as drain and source electrodes (for all organic devices), and finally, the optimization of the dip coating process by varying the coating speed, angle and environment. Also, OFETs are in fact most of the time thin-film transistors; thus, it is desirable to investigate film thickness properties during the study of processing techniques.

References

[1] M. Pope, H. P. Kallmann, and P. Magnante, "Electroluminescence in Organic Crystals," *The Journal of Chemical Physics,* vol. 38, pp. 2042-2043, 1963.

[2] C. K. Chiang, C. R. Fincher, Y. W. Park, A. J. Heeger, H. Shirakawa, E. J. Louis, S. C. Gau, and A. G. MacDiarmid, "Electrical Conductivity in Doped Polyacetylene," *Physical Review Letters,* vol. 39, p. 1098, 1977.

[3] C. W. Tang, S. A. VanSlyke, and C. H. Chen, "Electroluminescence of doped organic thin films," *Journal of Applied Physics,* vol. 65, pp. 3610-16, 1989.

[4] C. W. Tang and S. A. VanSlyke, "Organic electroluminescent diodes," *Applied Physics Letters,* vol. 51, pp. 913-15, 1987.

[5] H. Koezuka, A. Tsumura, and T. Ando, "Field-effect transistor with polythiophene thin film," Kyoto, Japan, 1987, pp. 699-704.

[6] A. Assadi, C. Svensson, M. Willander, and O. Inganas, "Field-effect mobility of poly(3-hexylthiophene)," *Applied Physics Letters,* vol. 53, pp. 195-7, 1988.

[7] W. Kobel, H. Kiess, and M. Egli, "Generation of micropatterns in poly(3-methyl-thiophene) films using microlithography: a first step in the design of an all-organic thin-film transistor," *Synthetic Metals,* vol. 22, pp. 265-71, 1988.

[8] A. Tsumura, H. Koezuka, and T. Ando, "Polythiophene field-effect transistor: its characteristics and operation mechanism," *Synthetic Metals,* vol. 25, pp. 11-23, 1988.

[9] R. A. Laudise, C. Kloc, P. G. Simpkins, and T. Siegrist, "Physical vapor growth of organic semiconductors," *Journal of Crystal Growth,* vol. 187, pp. 449-454, 1998.

[10] C. Kloc, P. G. Simpkins, T. Siegrist, and R. A. Laudise, "Physical vapor growth of centimeter-sized crystals of [alpha]-hexathiophene," *Journal of Crystal Growth,* vol. 182, pp. 416-427, 1997.

[11] R. W. I. De Boer, M. E. Gershenson, A. F. Morpurgo, and V. Podzorov, "Organic single-crystal field-effect transistors," *Physica Status Solidi (A) Applied Research,* vol. 201, pp. 1302-1331, 2004.

[12] C. Reese and Z. Bao, "Organic single-crystal field-effect transistors," *Materials Today,* vol. 10, pp. 20-27, 2007.

[13] V. Podzorov, E. Menard, A. Borissov, V. Kiryukhin, J. A. Rogers, and M. E. Gershenson, "Intrinsic charge transport on the surface of organic semiconductors," *Physical Review Letters,* vol. 93, pp. 086602-1, 2004.

[14] J. Takeya, M. Yamagishi, Y. Tominari, R. Hirahara, Y. Nakazawa, T. Nishikawa, T. Kawase, T. Shimoda, and S. Ogawa, "Very high-mobility organic single-crystal transistors with in-crystal conduction channels," *Applied Physics Letters,* vol. 90, pp. 102120-1, 2007.

[15] A. Salleo, "Charge transport in polymeric transistors," *Materials Today,* vol. 10, pp. 38-45, 2007.

[16] I. McCulloch, M. Heeney, C. Bailey, K. Genevicius, I. MacDonald, M. Shkunov, D. Sparrowe, S. Tierney, R. Wagner, Z. Weimin, M. L. Chabinyc, R. Joseph Kline, M. D. McGehee, and M. F. Toney, "Liquid-crystalline semiconducting polymers with high charge-carrier mobility," *Nature Materials,* vol. 5, pp. 328-33, 2006.

[17] T. Holstein, "Studies of polaron motion -- 1," *Annals of Physics,* vol. 8, pp. 325-389, 1959.

[18] T. Holstein, "Studies of polaron motion -- 2," *Annals of Physics,* vol. 8, pp. 325-389, 1959.

[19] P. G. Le Comber and W. E. Spear, "Electronic transport in amorphous silicon films," *Physical Review Letters,* vol. 25, pp. 509-11, 1970.

[20] J. Frenkel, "Theory of electric breakdown of dielectrics and electronic semiconductors," *Technical Physics of the USSR,* vol. 5, pp. 685-695, 1938.

[21] V. Coropceanu, J. Cornil, D. A. da Silva Filho, Y. Olivier, R. Silbey, and J.-L. Bredas, "Charge transport in organic semiconductors," *Chemical Reviews,* vol. 107, pp. 926-952, 2007.

[22] P. W. M. Blom, M. J. M. de Jong, and J. J. M. Vleggaar, "Electron and hole transport in poly(p-phenylene vinylene) devices," *Applied Physics Letters,* vol. 68, p. 3308, 1996.

[23] IEEE, "1640 IEEE Standart Test Methods for the Charaterization of Organic Transistors and Materials," 2004.

[24] P. K. Weimer, "TFT -- New thin-film transistor," *Institute of Radio Engineers -- Proceedings,* vol. 50, pp. 1462-1469, 1962.

[25] Y. Xia and G. M. Whitesides, "Soft lithography." vol. 28: Annual Reviews Inc, Palo Alto, CA, USA, 1998, pp. 153-184.

[26] K. Tamada, J. Nagasawa, F. Nakanishi, K. Abe, M. Hara, W. Knoll, T. Ishida, H. Fukushima, S. Miyashita, T. Usui, T. Koini, and T. R. Lee, "Structure of SAMs generated from functionalized thiols on gold," *Thin Solid Films,* vol. 327-329, pp. 150-155, 1998.

[27] S. Frey, A. Shaporenko, M. Zharnikov, P. Harder, and D. L. Allara, "Self-assembled monolayers of nitrile-functionalized alkanethiols on gold and silver substrates," *Journal of Physical Chemistry B,* vol. 107, pp. 7716-25, 2003.

[28] H. Fukushima, S. Seki, T. Nishikawa, H. Takiguchi, K. Tamada, K. Abe, R. Colorado, Jr., M. Graupe, O. E. Shmakova, and T. R. Lee, "Microstructure, wettability, and thermal stability of semifluorinated self-assembled monolayers (SAMs) on gold," *Journal of Physical Chemistry B,* vol. 104, pp. 7417-7423, 2000.

[29] V. Ganesh, S. K. Pal, S. Kumar, and V. Lakshminarayanan, "Self-assembled monolayers (SAMs) of alkoxycyanobiphenyl thiols on gold surface using a lyotropic liquid crystalline medium," *Electrochimica Acta,* vol. 52, pp. 2987-2997, 2007.

[30] D. Li and L. J. Guo, "Micron-scale organic thin film transistors with conducting polymer electrodes patterned by polymer inking and stamping," *Applied Physics Letters,* vol. 88, p. 063513, 2006.

[31] T. Granlund, T. Nyberg, L. S. Roman, M. Svensson, and O. Inganas, "Patterning of polymer light-emitting diodes with soft lithography," *Advanced Materials,* vol. 12, pp. 269-273, 2000.

[32] C. Kirkland, "SUPER-PRECISION DISC MOLDING: A NEW CHALLENGE TO PROCESSORS," *Plastics Technology,* vol. 31, pp. 73-82, 1985.

[33] L. Losner and A. S. Voloshin, "Compact disc quality control using digital image processing," *NDT International,* vol. 23, pp. 147-151, 1990.

[34] W. Michaeli and D. Opfermann, "Micro assembly injection moulding," *Microsystem Technologies,* vol. 12, pp. 616-19, 2006.

[35] G. Christian, "Injection Moulding of Parts with Microstructured Surfaces for Medical Applications," *Macromolecular Symposia,* vol. 217, pp. 365-374, 2004.

[36] F. Nikolajeff, S. Jacobsson, S. Hard, B. Billman, L. Lundbladh, and C. Lindell, "Replication of continuous-relief diffractive optical elements by conventional compact disc injection-molding techniques," *Applied Optics,* vol. 36, pp. 4655-9, 1997.

[37] Y. Xia, J. J. McClelland, R. Gupta, D. Qin, X. M. Zhao, L. L. Sohn, R. J. Celotta, and G. M. Whitesides, "Replica molding using polymeric materials: A practical step toward nanomanufacturing," *Advanced Materials,* vol. 9, pp. 147-149, 1997.

[38] X. Younan, K. Enoch, Z. Xiao-Mei, J. A. Rogers, M. Prentiss, and G. M. Whitesides, "Complex optical surfaces formed by replica molding against elastomeric masters," *Science,* vol. 273, pp. 347-9, 1996.

[39] C. K. Y. Wong, O. C. T. Cheung, B. Xu, and M. M. F. Yuen, "Using PDMS microtransfer molding (μTM) for polymer flip chip," New Orleans LA, United States, 2003, pp. 652-657.

[40] W. Y. Leung, H. Kang, K. Constant, D. Cann, C. H. Kim, R. Biswas, M. M. Sigalas, and K. M. Ho, "Fabrication of photonic band gap crystal using microtransfer molded templates," *Journal of Applied Physics,* vol. 93, pp. 5866-5870, 2003.

[41] X.-M. Zhao, S. P. Smith, S. J. Waldman, G. M. Whitesides, and M. Prentiss, "Demonstration of waveguide couplers fabricated using microtransfer molding," *Applied Physics Letters,* vol. 71, pp. 1017-1019, 1997.

[42] J. Hu, T. Deng, R. G. Beck, R. M. Westervelt, and G. M. Whitesides, "Fabrication of arrays of Schottky diodes using microtransfer molding," *Sensors and Actuators, A: Physical,* vol. 75, pp. 65-69, 1999.

[43] H.-C. Jin, J. R. Abelson, M. K. Erhardt, and R. G. Nuzzo, "Soft lithographic fabrication of an image sensor array on a curved substrate," *Journal of Vacuum Science and Technology B: Microelectronics and Nanometer Structures,* vol. 22, pp. 2548-2551, 2004.

[44] Z. Fengling, T. Nyberg, and O. Inganas, "Conducting polymer nanowires and nanodots made with soft lithography," *Nano Letters,* vol. 2, pp. 1373-7, 2002.

[45] A. Blumel, A. Klug, S. Eder, U. Scherf, E. Moderegger, and E. J. W. List, "Micromolding in capillaries and microtransfer printing of silver nanoparticles as soft-lithographic approach for the fabrication of source/drain electrodes in organic field-effect transistors," *Organic Electronics: physics, materials, applications,* vol. 8, pp. 389-395, 2007.

[46] A. C. Arias, S. E. Ready, R. Lujan, W. S. Wong, K. E. Paul, A. Salleo, M. L. Chabinyc, R. Apte, R. A. Street, Y. Wu, P. Liu, and B. Ong, "All jet-printed polymer thin-film transistor active-matrix backplanes," *Applied Physics Letters,* vol. 85, pp. 3304-6, 2004.

[47] B. Ballarin, A. Fraleoni-Morgera, D. Frascaro, S. Marazzita, C. Piana, and L. Setti, "Thermal inkJet microdeposition of PEDOT:PSS on ITO-coated glass and characterization of the obtained film," *Synthetic Metals,* vol. 146, pp. 201-205, 2004.

[48] S. E. Burns, P. Cain, J. Mills, J. Wang, and H. Sirringhaus, "Inkjet Printing of Polymer Thin-Film Transistor Circuits," *MRS Bulletin,* vol. 28, pp. 829-834, 2003.

[49] B. Chen, T. Cui, Y. Liu, and K. Varahramyan, "All-polymer RC filter circuits fabricated with inkjet printing technology," *Solid-State Electronics,* vol. 47, pp. 841-847, 2003.

[50] T. Kawase, H. Sirringhaus, R. H. Friend, and T. Shimoda, "All-polymer thin film transistors fabricated by inkjet printing," San Diego, CA, USA, 2001, pp. 80-8.

[51] T. Shimoda and T. Kawase, "All-polymer thin film transistor fabricated by high-resolution ink-jet printing," San Francisco, CA., United States, 2003, pp. 285-287.

[52] T. Shimoda, K. Morii, S. Seki, and H. Kiguchi, "Inkjet Printing of Light-Emitting Polymer Displays," *MRS Bulletin,* vol. 28, pp. 821-827, 2003.

[53] I. Takasu, K. Sugi, Y. Nomura, H. Nakao, K. Mori, I. Amemiya, and S. Uchikoga, "All-solution-processed organic thin film transistors fabricated by non-piezoelectric Inkjet printing," Cancun, Mexico, 2006, pp. 307-312.

[54] Y. Yang and J. Bharathan, "Ink-jet printing technology and its application in polymer multicolor EL displays," Anaheim, CA, USA, 1998, pp. 19-21.

[55] F. Y. Gan, "Thin film transistors with chemically deposited active channels," 2001, pp. xv, 170 leaves.

[56] D. B. A. Rep, A. F. Morpurgo, and T. M. Klapwijk, "Doping-dependent charge injection into regioregular poly(3-hexylthiophene)," *Organic Electronics,* vol. 4, pp. 201-7, 2003.

[57] A. L. Briseno, M. Roberts, M.-M. Ling, H. Moon, E. J. Nemanick, and Z. Bao, "Patterning organic semiconductors using "dry" poly(dimethylsiloxane) elastomeric stamps for thin film transistors," *Journal of the American Chemical Society,* vol. 128, pp. 3880-3881, 2006.

[58] X. Wang, M. Ostblom, T. Johansson, and O. Inganas, "PEDOT surface energy pattern controls fluorescent polymer deposition by dewetting," *Thin Solid Films,* vol. 449, pp. 125-32, 2004.

[59] K. Glasmastar, J. Gold, A.-S. Andersson, D. S. Sutherland, and B. Kasemo, "Silicone transfer during microcontact printing," *Langmuir,* vol. 19, pp. 5475-5483, 2003.

[60] D. J. Graham, D. D. Price, and B. D. Ratner, "Solution assembled and microcontact printed monolayers of dodecanethiol on gold: A multivariate exploration of chemistry and contamination," *Langmuir,* vol. 18, pp. 1518-1527, 2002.

[61] J.-F. Chang, B. Sun, D. W. Breiby, M. M. Nielsen, T. I. Solling, M. Giles, I. McCulloch, and H. Sirringhaus, "Enhanced Mobility of poly(3-hexylthiophene) transistors by spin-coating from high-boiling-point solvents," *Chemistry of Materials,* vol. 16, pp. 4772-4776, 2004.

[62] Y. Chen, I. Shih, and S. Xiao, "Effects of FeCl[sub 3] doping on polymer-based thin film transistors," *Journal of Applied Physics,* vol. 96, pp. 454-458, 2004.

[63] M. S. A. Abdou, F. P. Orfino, Y. Son, and S. Holdcroft, "Interaction of oxygen with conjugated polymers: Charge transfer complex formation with poly(3-alkylthiophenes)," *Journal of the American Chemical Society,* vol. 119, p. 4518, 1997.

[64] G. Wang, T. Hirasa, D. Moses, and A. J. Heeger, "Fabrication of regioregular poly(3-hexylthiophene) field-effect transistors by dip-coating," *Synthetic Metals,* vol. 146, pp. 127-132, 2004.

[65] G. Wang, J. Swensen, D. Moses, and A. J. Heeger, "Increased mobility from regioregular poly(3-hexylthiophene) field-effect transistors," *Journal of Applied Physics,* vol. 93, pp. 6137-6141, 2003.

[66] S. Cho, K. Lee, J. Yuen, G. Wang, D. Moses, A. J. Heeger, M. Surin, and R. Lazzaroni, "Thermal annealing-induced enhancement of the field-effect mobility of regioregular poly(3-hexylthiophene) films," *Journal of Applied Physics,* vol. 100, pp. 114503-6, 2006.

[67] E. Menard, V. Podzorov, S.-H. Hur, A. Gaur, M. E. Gershenson, and J. A. Rogers, "High-performance n- And p-type single-crystal organic transistors with free-space gate dielectrics," *Advanced Materials,* vol. 16, pp. 2097-2101, 2004.